AN IRREGULARLY PORTIONED FDF SOLVER FOR TURBULENT FLOW SIMULATION

by

Patrick H. Pisciuneri

Submitted to the Graduate Faculty of
the Swanson School of Engineering in partial fulfillment
of the requirements for the degree of
Doctor of Philosophy

University of Pittsburgh

2013

UNIVERSITY OF PITTSBURGH

SWANSON SCHOOL OF ENGINEERING

This dissertation was presented

by

Patrick H. Pisciuneri

It was defended on

July 16, 2013

and approved by

Peyman Givi, Ph.D., James T. MacLeod Professor of Mechanical Engineering and Materials Science, Professor of Chemical and Petroleum Engineering

William S. Slaughter, Ph.D., Associate Professor of Mechanical Engineering and Materials Science

Albert C. To, Ph.D., Assistant Professor of Mechanical Engineering and Materials Science

Nadine Aubry, Ph.D., Dean of the College of Engineering, Northeastern University

Dissertation Director: Peyman Givi, Ph.D., James T. MacLeod Professor of Mechanical Engineering and Materials Science, Professor of Chemical and Petroleum Engineering

AN IRREGULARLY PORTIONED FDF SOLVER FOR TURBULENT FLOW SIMULATION

Patrick H. Pisciuneri, PhD

University of Pittsburgh, 2013

A new computational methodology is developed for large eddy simulation (LES) with the filtered density function (FDF) formulation of turbulent reacting flows. This methodology is termed the "irregularly portioned Lagrangian Monte Carlo finite difference" (IPLMCFD). It takes advantage of modern parallel platforms and mitigates the computational cost of LES/FDF significantly. The embedded algorithm addresses the load balancing issue by decomposing the computational domain into a series of irregularly shaped and sized subdomains. The resulting algorithm scales to thousands of processors with an excellent efficiency. Thus it is well suited for LES of reacting flows in large computational domains and under complex chemical kinetics. The efficiency of the IPLMCFD; and the realizability, consistency and the predictive capability of FDF are demonstrated by LES of several turbulent flames.

TABLE OF CONTENTS

LIST OF TABLES

LIST OF FIGURES

PREFACE

Modeling of turbulent reacting flows requires knowledge in many areas including transport phenomena, chemical kinetics and applied mathematics. Numerical simulation of such flows requires knowledge of numerical methods, computational algorithms; and as I hope to convince you in this work, parallel programming and high performance computing. Studying such a broad range of subjects has been exciting and overwhelming; but also rewarding. The fact that I made it this far is a testament to all the help that I received along the way.

I am sincerely grateful to my adviser, Professor Peyman Givi, for providing me this opportunity, and for his support, guidance and patience during my graduate studies. I would like to thank the members of my doctoral committee, Professors Nadine Aubry, William Slaughter and Albert To. Also, I would like to thank Professor Cyrus Madnia of the University at Buffalo. It has been a pleasure to collaborate and interact with his group. And I am grateful to Dr. Peter Strakey and Dr. Nathan Weiland of the National Energy Technology Laboratory, who have provided support and firsthand insight into many physical aspects of turbulent combustion.

I would also like to thank all of my colleagues that I had the pleasure to work with at one point or another during my time at the Laboratory for Computational Transport Phenomena at the University of Pittsburgh: Dr. Naseem Ansari, Dr. Tomasz Drozda, Dr. Mahdi Mohebbi, Dr. Mehdi Nik, Dr. Collin Otis, Mr. Sasan Salkhordeh, Dr. Reza Sheikhi and Dr. Levent Yilmaz. I am particularly grateful to Drs. Nik, Sheikhi and Yilmaz, who mentored me and showed me how to be successful as a new member of the group.

Most importantly, I would like to acknowledge my entire family, particularly my mom & dad, my sister, Kellie, and my girlfriend, Noelle. They have provided love, support and patience throughout this endeavor. I cannot thank them enough, only I hope that I have grown into a better person during my time here at Pitt.

As part of the National Energy Technology Laboratory's Regional University Alliance (NETL-RUA), a collaborative initiative of the NETL, this technical effort was performed under the DOE-RES Contract DE-FE0004000. Additional support for this work is provided by AFOSR & NASA under Grant FA9550-09-1-0611, by AFOSR under Grant FA9550-12-1-0057, by NSF under Grant CBET-1250171, by the NSF Extreme Science and Engineering Discovery Environment (XSEDE) under Grants TG-CTS070055N & TG-CTS120015; and by the University of Pittsburgh Center for Simulation and Modeling.

PATRICK H. PISCIUNERI

UNIVERSITY OF PITTSBURGH, 2013

1.0 INTRODUCTION

The filtered density function (FDF) methodology [1] has proven to be very effective in the subgrid scale (SGS) modeling required for large eddy simulation (LES) of turbulent reacting flows. This methodology was first introduced by Givi [2] and then formally defined by Pope [3]. It is basically the counterpart to the probability density function (PDF) approach used in Reynolds averaged Navier-Stokes (RANS) simulations. The LES/FDF methodology is suited for the treatment of large-scale, unsteady phenomena. Thus, when compared to RANS, it provides a more detailed and reliable prediction of turbulent reacting flows [4].

The FDF has evolved extensively since its original conception. Colucci *et al.* [5] developed and solved the transport equation for the marginal scalar FDF (SFDF) suitable for constant density flows. The variable density formulation of the SFDF was developed by Jaberi *et al.* [6], and it is known as the scalar filtered mass density function (SFMDF). The marginal velocity FDF (VFDF) was developed by Gicquel *et al.* [7]. Joint velocity-scalar approaches have been developed for constant density (VSFDF) and variable density (VSFMDF) flows by Sheikhi *et al.* [8, 9]. The current state of the art for LES of low-speed flows is the frequency-velocity-scalar filtered mass density function (FVS-FMDF) and is due to Sheikhi *et al.* [10]. The most systematic means of LES of high-speed flows is via the energy-pressure-velocity-scalar filtered mass density function (EPVS-FMDF) and is due to Nik [11, 12].

Despite its popularity, a major challenge still associated with the LES/FDF methodology is its computational cost. This cost is exacerbated by the complexity of the chemical kinetics. For moderately sized geometries with even reduced finite-rate kinetics simulations can take on the order of a few years [13].

1.1 SGS CLOSURE IN TURBULENT COMBUSTION

The filtering operation in LES results in the subgrid scale (SGS) closure problem [2, 14]. This problem, particularly in regards to the chemical source term, has been the subject of broad investigation, resulting in a variety of approaches [1, 15–20]. Typically, most models are based on those which have shown success in RANS.

Combustion modes are often split into two categories [21]: nonpremixed and premixed. It is helpful to differentiate between these two regimes as some of the models are for one particular regime or the other. In nonpremixed combustion, the fuel and air streams are introduced separately. Combustion occurs after the onset of mixing by molecular diffusion. Thus, sometimes the label "diffusion flame" is adopted for this mode. Premixed flames provide a mixture of fuel and oxidizer prior to entry into the combustor. They offer the advantage of greater control over the reacting mixture. However, greater care is required in the design of premixed combustors, as the mixture is volatile.

These two regimes are not entirely separate, as in most cases, the mode is via partially premixed combustion. An example is a lifted flame. In such flames, fuel and air are separately inserted into the combustor, as in the nonpremixed case. However, under suitable conditions [22] if the flame is lifted from the burner, mixing of the fuel and air occurs before combustion, as in the premixed case.

A survey of combustion literature reveals significant progress in LES of reacting turbulent flows. It appears that Schumann [23] was one of the first to conduct LES of a reacting flow. However, the assumption made in this work to simply neglect the contribution of SGS scalar fluctuations to the filtered reaction rate is debatable. The importance of such fluctuations has been long recognized in RANS in both combustion [24] and chemical engineering [25, 26]. To account for such fluctuations, significant progress has been made within the past 25 years. In the next two sections, a review is made of some of the more widely used closures in both combustion regimes.

1.2 SGS CLOSURES IN NONPREMIXED FLAMES

The obvious extension of Schumann's method is to develop and solve transport equations for the SGS higher order moments [27, 28]. These methods are not very powerful as the number of moments to be considered does not converge. This is similar to the classical closure problem in turbulence [29–31]. One remedy for this problem is to use PDF methods. These methods go back to the pioneering work of Toor [32] and have been widely used in RANS [2, 3, 33–37]. This approach offers the advantage that all the statistical information pertaining to the scalar field is embedded within the PDF. Therefore, once the PDF is known the effects of scalar fluctuations are easily determined.

A systematic approach for determining the SGS-PDF is by means of solving the transport equation governing its evolution [38, 39]. In this equation the effects of chemical reactions appear in a closed form. However, modeling is needed to account for transport of the PDF in the domain of the random variables. This transport describes the role of molecular action on the evolution of PDF. In addition, there is an extra dimensionality associated with the composition domain which must be treated. These problems have constituted a stumbling block in utilizing PDF methods in practical applications. Developments of turbulence closures and numerical schemes which can effectively deal with these predicaments have been the subject of broad investigations within the past two decades.

An alternative approach in PDF modeling is based on *assumed* methods. In these methods the PDF is not determined by solving a transport equation. Rather, its shape is assumed *a priori* usually in terms of the low order moments of the random variable(s). Obviously, this method is *ad hoc* but it offers more flexibility than the first approach. This approach is pioneered by Madnia *et al.* [27, 40].

The assumed PDF method is typically used in conjunction with the "infinitely fast" and/or chemical equilibrium model. With this model, it is possible to relate the thermochemical variables to the mixture fraction (ξ). This is a "conserved" scalar variable, thus there is no closure problem associated with its chemical source term. When chemistry is assumed to be single-step and irreversible, the resulting "Burke-Schumann" flame structure

[41–44] is easily described: When $\xi < \xi_{st}$:

$$Y_F = 0, \qquad Y_O = Y_O^0 \left(1 - \frac{\xi}{\xi_{st}}\right), \tag{1.1}$$

$$T = \xi T_F^0 + (1-\xi) T_O^0 + \Delta Q Y_F^0 \xi, \tag{1.2}$$

and when $\xi \geq \xi_{st}$:

$$Y_F = Y_F^0 \frac{\xi - \xi_{st}}{1 - \xi_{st}}, \qquad Y_O = 0, \tag{1.3}$$

$$T = \xi T_F^0 + (1-\xi) T_O^0 + \Delta Q Y_F^0 \xi_{st} \frac{1-\xi}{1-\xi_{st}}, \tag{1.4}$$

where ξ_{st} is the stoichiometric mixture fraction, Y_F and Y_O are the fuel and oxidizer mass fractions and T is the temperature. Additionally, Y_F^0 and T_F^0 are the fuel mass fraction and temperature in the fuel stream, Y_O^0 and T_O^0 are the oxidizer mass fraction and temperature in the oxidizer stream, and ΔQ is the heat release parameter. Therefore, with this assumption there is no fuel present when the mixture fraction is less than stoichiometric and no oxidizer when the mixture fraction is greater than stoichiometric. At the stoichiometric mixture fraction fuel and oxidizer are both zero and the mixture is entirely composed of products.

When *some* non-equilibrium effects are present, the *flamelet* approach is more appropriate. In this case, all the thermochemical variables are parameterized in terms of the mixture fraction and its rate of dissipation (χ). A laminar diffusion flamelet is defined as the region in the vicinity of the stoichiometric mixture fraction surface when the mixture fraction has a high gradient. This concept was developed into a combustion model by Peters [45]. The resulting flamelet equations are [44]:

$$\rho \frac{\partial \phi}{\partial t} = \frac{1}{2} \rho \chi \frac{\partial^2 \phi}{\partial \xi^2} + \dot{\omega}_\phi, \tag{1.5}$$

where ϕ indicates a reactive scalar variable, ρ the density and $\dot{\omega}_\phi$ the chemical source term. The mixture fraction dissipation (strain) rate is given by:

$$\chi = 2D \left(\frac{\partial \xi}{\partial x_i} \frac{\partial \xi}{\partial x_i}\right), \tag{1.6}$$

where D is the diffusion coefficient and x_i $(i = 1, 2, 3)$ and t represent space and time, respectively. Equation (1.5) comprises the unsteady flamelet equation. It can be solved

numerically over the entire mixture fraction space with the use of proper chemical kinetics models, and the results stored in a table. Then coupling the thermochemistry with hydrodynamics involves looking up the tabulated composition based on the mixture fraction. When the time dependent term in Eq. (1.5) is ignored, it yields the steady flamelet model. The flamelet approach coupled with PDF methods has experienced some success [46–54].

Another methodology coupled with assumed PDF is the conditional moment closure (CMC). This closure is originally due to Klimenko [55] and Bilger [56] and considers the conditional averages of the thermodynamic variables. The resulting equations feature the reaction source term conditioned on the mixture fraction. Typically, this term is approximated by using the mean conditional mass fractions and conditional temperature. This is referred to as first-order CMC, as the higher order conditional moments are neglected. The CMC approach has shown some progress for LES [57–65].

A somewhat similar and newer approach is that of multiple mapping conditioning (MMC). This method is developed by Klimenko and Pope [66] and unifies the CMC and PDF approaches. In the MMC method, the governing equations are conditioned on a subset of reference variables, N_m, where $1 < N_m < N_s$ and N_s is the number of species describing the thermochemistry, which can be extended to include quantities such as the mixture fraction and the scalar dissipation. The composition is then represented by the joint PDF of the reference variables, and the means of the remaining species conditioned on the reference variables, for which a transport equation is constructed. The benefit is that it is not necessary to construct a joint PDF of dimension N_s which can be expensive. Also, a well chosen set of reference variables should yield better result than the traditional CMC methods.

Most of the previous work based on these models make the assumption of a β-density for the SGS-PDF of the mixture fraction. This requires knowledge of the first two moments of the mixture fraction [27, 67]. The β-density coupled with the assumption of flame sheet model has been applied for LES of a variety of turbulent flames [40, 68]. It has also been coupled with the flamelet assumption [50, 69]. An obvious drawback of the approach is that the assumed shape of the PDF is only valid for a conserved scalar, such as the mixture fraction [70]. Also, the mixture fraction coupled with the steady flamelet assumption cannot account for unsteady flame dynamics, such as ignition and extinction. Pierce and Moin

[71] have developed and demonstrated a combined flamelet/progress variable approach to capture unsteady phenomena. This methodology has been applied for the LES of gas turbine combustors [72, 73].

The linear-eddy model (LEM) is a one-dimensional mixing and reacting closure originally due to Kerstein [74–78]. Implementation for LES involves two steps. The first is a turbulent stirring mechanism, modeled by a rearrangement of the scalar field according to the *triplet map*. This represents the effect of turbulent mixing on the SGS due to a vortex of size l, with $\eta < l < \Delta$, where η is the Kolmogorov length scale and Δ the LES filter size. The second step is the solution of a one-dimensional unsteady diffusion-reaction equation:

$$\frac{\partial \rho Y_\alpha}{\partial t} = \frac{\partial}{\partial x}\left(\rho D_\alpha \frac{\partial Y_\alpha}{\partial x}\right) + \dot{\omega}_\alpha, \qquad \alpha = 1, 2, \ldots, N_s, \tag{1.7}$$

where Y_α is the mass fraction of species α. In this context, one could consider complex chemical kinetics for the evaluation of $\dot{\omega}_\alpha$ or the effects of differential diffusion ($D_\alpha \neq D$). The LEM has been employed for the LES of many reacting flows [15, 79, 80]. The extension of the method known as one-dimensional turbulence (ODT) [81–83] has also been used extensively for LES [84–91].

1.3 SGS CLOSURES IN PREMIXED FLAMES

Premixed flames present a challenge for LES because the thickness of the flame is usually smaller than the LES grid size [44]. Thus approaches are usually based on an artificially thickened flame front, tracking the location of a flame front, or in the most simple case, by ignoring this fact altogether. Some of the SGS closures which are used for LES of premixed flames are discussed here.

The eddy-break-up model in RANS is a simple concept and ignores the flame thickness problem [92, 93]. In this approach, the reaction rate is defined in terms of the *progress variable*, typically a reduced temperature which ranges from zero in the fresh gases to one in the fully burned gases, and a characteristic SGS time scale. An example of its usage for LES is given by Fureby and Löfström [94].

Another popular methodology is the thickened flame model [95]. In this model, the idea is to consider a flame with the same laminar flame speed as the actual flame, but is artificially thickened in such a way that the combustion zone is resolvable by the computational grid. A detailed discussion of this approach, and its application to LES are given in Refs. [96–102].

Alternatively to the thickened flame model, in the the G-equation model, the flame thickness can be considered negligible. In this case, the flame front is associated with an isosurface, $G = G_0$ [44, 103]. A transport equation for the propagation of this surface is solved. Values of $G > G_0$ represent fully burned gases and values of $G < G_0$ represent unburned gases [18]. Further details of this approach and application in the context of LES are given in Refs. [104–109].

1.4 OBJECTIVE AND SCOPE

Most of the models presented for closure of the reaction source term in LES have a limited range of applicability. For example, *a priori* assumptions about the speed of the chemistry must be made, or at the very least hinted at by experimental data if it is available. When the underlying assumptions are valid, the model may yield excellent predictions. But what if there are no experimental data to validate the assumptions? What if the experiment becomes replaced by the simulation? What if the most accurate means of prediction is required?

We feel that the transported PDF methodology provides the most optimum means of LES of reacting flows. Since this original work, the FDF has experienced widespread usage, and is now regarded as one of the most effective and popular means of LES worldwide. Some of the most noticeable contributions in FDF by others are in its basic implementation [110–124], fine-tuning of its sub-closures [125–127] and its validation via laboratory experiments [114, 128–132]. For a review of the state of progress in FDF modeling we refer to [4]. For a comprehensive understanding of the FDF, we refer serious readers to several previous dissertations [12, 133–140].

The work presented in this dissertation describes the development of a *robust* LES/FDF solution technique. The objective is to make FDF simulations for reacting flows practical

through the development of a highly scalable computational algorithm. The new computational methodology is implemented via the employment of the SFMDF and is assessed in terms of its performance and overall capability.

Chapter 2 describes the new algorithm, its scalability and realizability, along with the simulation results establishing its consistency and reliability. Chapter 3 provides conclusions and some suggestions for future work. The materials in Chapter 2 is to be published in *SIAM J. Sci. Comput.* [141]. Also, it has been presented at the last two APS-DFD meetings [142, 143]. This dissertation has been an integral part of an invited AIAA lecture [144], and an upcoming invited lead article [145]. Several elements of this dissertation contributed to other publications by the author [146, 147].

2.0 IRREGULARLY PORTIONED FDF SIMULATOR

A new computational methodology, termed "irregularly portioned Lagrangian Monte Carlo finite difference" (IPLMCFD), is developed for large eddy simulation (LES) of turbulent combustion via the filtered density function (FDF). This is a hybrid methodology which couples a Monte Carlo FDF simulator with a structured Eulerian finite difference LES solver. The IPLMCFD is scalable to thousands of processors; thus is suited for simulation of complex reactive flows. The scalability & consistency of the hybrid solver and the realizability & reliability of the generated results are demonstrated via LES of several turbulent flames under both nonpremixed and premixed conditions.

2.1 GOVERNING EQUATIONS

For low-speed compressible flows with chemical reaction, the primary transport variables are the density, $\rho(\mathbf{x},t)$, the velocity vector, $u_i(\mathbf{x},t)$ $(i=1,2,3)$, the pressure, $p(\mathbf{x},t)$, the total specific enthalpy, $h(\mathbf{x},t)$, and the species mass fractions, $Y_\alpha(\mathbf{x},t)$ $(\alpha=1,2,\ldots,N_s)$ where N_s is the number of species. The equations which govern the transport of these variables in space ($x_i,\ i=1,2,3$) and time (t) are the continuity, momentum, species mass conservation and enthalpy equations, along with an equation of state:

$$\frac{\partial \rho}{\partial t}+\frac{\partial \rho u_i}{\partial x_i}=0, \tag{2.1}$$

$$\frac{\partial \rho u_j}{\partial t}+\frac{\partial \rho u_i u_j}{\partial x_i}=-\frac{\partial p}{\partial x_j}+\frac{\partial \tau_{ij}}{\partial x_i}, \tag{2.2}$$

$$\frac{\partial \rho \phi_\alpha}{\partial t} + \frac{\partial \rho u_i \phi_\alpha}{\partial x_i} = -\frac{\partial J_i^\alpha}{\partial x_i} + \rho S_\alpha, \qquad \alpha = 1, 2, \ldots, N_s, \sigma = h, \tag{2.3}$$

$$p = \rho R_u T \sum_{\alpha=1}^{N_s} Y_\alpha / M_\alpha = \rho R T, \tag{2.4}$$

where R_u and R are the universal and mixture gas constants respectively, and M_α is the molecular weight of species α. Equation (2.3) presents species mass conservation and the transport of enthalpy in a common form, with the composition, $\boldsymbol{\phi}(\mathbf{x}, t)$, defined as:

$$\phi_\alpha = Y_\alpha, \ \alpha = 1, 2, \ldots, N_s, \qquad \phi_\sigma = h. \tag{2.5}$$

The chemical source terms are functions of the composition variables only, $S_\alpha = S_\alpha(\boldsymbol{\phi})$. For a Newtonian fluid with Fickian diffusion, the viscous stress tensor (τ_{ij}), and the mass and heat flux (J_i^α) are given by:

$$\tau_{ij} = \mu \left(\frac{\partial u_i}{\partial x_j} + \frac{\partial u_j}{\partial x_i} - \frac{2}{3} \delta_{ij} \frac{\partial u_k}{\partial x_k} \right), \tag{2.6}$$

$$J_i^\alpha = -\gamma \frac{\partial \phi_\alpha}{\partial x_i}, \tag{2.7}$$

where μ is the dynamic viscosity and $\gamma = \rho\Gamma$ denotes the thermal and mass molecular diffusivity coefficients. Large eddy simulation involves the spatial filtering operation [14, 148]:

$$\langle Q(\mathbf{x}, t) \rangle_\ell = \int_{-\infty}^{+\infty} Q(\mathbf{x}', t) \mathcal{G}(\mathbf{x}', \mathbf{x}) \mathrm{d}\mathbf{x}', \tag{2.8}$$

where $\mathcal{G}$ denotes a filter function of width Δ_G and $\langle Q(\mathbf{x}, t) \rangle_\ell$ is the filtered value of the transport variable, $Q(\mathbf{x}, t)$. For variable density flows, it is convenient to consider the Favre filtered quantity, defined as $\langle Q(\mathbf{x}, t) \rangle_L = \langle \rho Q \rangle_\ell / \langle \rho \rangle_\ell$. We consider a filter function that is localized and spatially and temporally invariant, $\mathcal{G}(\mathbf{x}', \mathbf{x}) \equiv G(\mathbf{x}' - \mathbf{x})$, with the properties $G(\mathbf{x}) = G(-\mathbf{x})$ and $\int_{-\infty}^{+\infty} G(\mathbf{x}) \mathrm{d}\mathbf{x} = 1$. Moreover, only a "positive" filter function as defined by Vreman *et al.* [149] is considered for which all of the moments $\int_{-\infty}^{+\infty} x^m G(x) \mathrm{d}x = 1$ exist for $m \geq 0$. Applying the filtering operation to Eqs. (2.1 - 2.4):

$$\frac{\partial \langle \rho \rangle_\ell}{\partial t} + \frac{\partial \langle \rho \rangle_\ell \langle u_i \rangle_L}{\partial x_i} = 0, \tag{2.9}$$

$$\frac{\partial \langle\rho\rangle_\ell \langle u_j\rangle_L}{\partial t} + \frac{\partial \langle\rho\rangle_\ell \langle u_i\rangle_L \langle u_j\rangle_L}{\partial x_i} = -\frac{\partial \langle p\rangle_\ell}{\partial x_j} + \frac{\partial \langle\tau_{ij}\rangle_\ell}{\partial x_i} - \frac{\partial T_{ij}}{\partial x_i}, \tag{2.10}$$

$$\frac{\partial \langle\rho\rangle_\ell \langle\phi_\alpha\rangle_L}{\partial t} + \frac{\partial \langle\rho\rangle_\ell \langle u_i\rangle_L \langle\phi_\alpha\rangle_L}{\partial x_i} = -\frac{\partial \langle J_i^\alpha\rangle_\ell}{\partial x_i} - \frac{\partial M_i^\alpha}{\partial x_i} + \langle\rho\rangle_\ell \langle S_\alpha\rangle_L, \tag{2.11}$$

$$\langle p\rangle_\ell = \langle\rho\rangle_\ell \langle RT\rangle_L, \tag{2.12}$$

where $T_{ij} = \langle\rho\rangle_\ell (\langle u_i u_j\rangle_L - \langle u_i\rangle_L \langle u_j\rangle_L)$ and $M_i^\alpha = \langle\rho\rangle_\ell (\langle u_i \phi_\alpha\rangle_L - \langle u_i\rangle_L \langle\phi_\alpha\rangle_L)$ denote the subgrid scale (SGS) stress and SGS mass flux, respectively.

2.2 SGS CLOSURE FOR HYDRODYNAMICS

The SGS closure problem for LES of non-reacting flows is due to T_{ij} and M_i^α [150]. In reacting flows, the filtered source terms, $\langle S_\alpha\rangle_L$, also require closure, which is the subject of FDF methodology presented in the next section. For T_{ij}, the modified kinetic energy viscosity (MKEV) model based on the work of Bardina *et al.* [151], and extended for compressible flows by Jaberi *et al.* [6] is used:

$$T_{ij} = -2C_R \langle\rho\rangle_\ell \Delta_G \mathcal{E}^{1/2} \left(\langle \mathcal{S}_{ij}\rangle_L - \frac{1}{3} \langle \mathcal{S}_{kk}\rangle_L \delta_{ij} \right) + \frac{2}{3} C_I \langle\rho\rangle_\ell \mathcal{E} \delta_{ij}, \tag{2.13}$$

where C_R and C_I are model constants. The resolved strain rate tensor is given by:

$$\langle \mathcal{S}_{ij}\rangle_L = \frac{1}{2} \left(\frac{\partial \langle u_i\rangle_L}{\partial x_j} + \frac{\partial \langle u_j\rangle_L}{\partial x_i} \right), \tag{2.14}$$

and the *modified kinetic energy*, $\mathcal{E}$, is:

$$\mathcal{E} = |\langle u_i^*\rangle_L \langle u_i^*\rangle_L - \langle\langle u_i^*\rangle_L\rangle_{\ell'} \langle\langle u_i^*\rangle_L\rangle_{\ell'}|, \tag{2.15}$$

with $u_i^* = u_i - \mathcal{U}_i$, where $\mathcal{U}_i$ is a reference velocity in the x_i direction. The subscript ℓ' denotes a filter at a secondary level of size $\Delta_{G'} > \Delta_G$. The SGS eddy viscosity is thus expressed as:

$$\nu_t = C_R \Delta_G \mathcal{E}^{1/2}. \tag{2.16}$$

The SGS mass fluxes, M_i^α, are modeled similarly [152],

$$M_i^\alpha = -\gamma_t \frac{\partial \langle \phi_\alpha \rangle_L}{\partial x_i}, \tag{2.17}$$

where $\gamma_t = \langle \rho \rangle_\ell \, \nu_t / Sc_t$ is the subgrid diffusivity, and Sc_t is the subgrid Schmidt number.

2.3 SFMDF

The SFMDF is defined as

$$F_L\left(\boldsymbol{\psi}; \mathbf{x}, t\right) = \int_{-\infty}^{+\infty} \rho\left(\mathbf{x}', t\right) \zeta\left[\boldsymbol{\psi}, \boldsymbol{\phi}\left(\mathbf{x}', t\right)\right] G(\mathbf{x}' - \mathbf{x}) \mathrm{d}\mathbf{x}', \tag{2.18}$$

where the "fine-grained" density is

$$\zeta\left[\boldsymbol{\psi}, \boldsymbol{\phi}\left(\mathbf{x}, t\right)\right] = \delta\left[\boldsymbol{\psi} - \boldsymbol{\phi}\left(\mathbf{x}, t\right)\right] \equiv \prod_{\alpha=1}^{\sigma} \delta\left[\psi_\alpha - \phi_\alpha\left(\mathbf{x}, t\right)\right]. \tag{2.19}$$

Here δ denotes the delta function and $\boldsymbol{\psi}$ the composition space of the scalar array ($\boldsymbol{\phi}$). The complete SGS statistical information for the scalars is contained within the SFMDF, and is governed by the transport equation [1]:

$$\begin{aligned} \frac{\partial F_L}{\partial t} + \frac{\partial \langle u_i \rangle_L F_L}{\partial x_i} &= \frac{\partial}{\partial x_i}\left[\left(\gamma + \gamma_t\right) \frac{\partial F_L / \langle \rho \rangle_\ell}{\partial x_i}\right] \\ &+ \frac{\partial}{\partial \psi_\alpha}\left[\Omega_m \left(\psi_\alpha - \langle \phi_\alpha \rangle_L\right) F_L\right] - \frac{\partial [S_\alpha F_L]}{\partial \psi_\alpha}, \end{aligned} \tag{2.20}$$

where γ_t represents the subgrid thermal and mass molecular diffusivity. The SGS mixing frequency, $\Omega_m = C_\Omega(\gamma + \gamma_t)/(\langle \rho \rangle_\ell \, \Delta_G^2)$, is due to the linear mean-square estimation (LMSE) [35, 153], where C_Ω is a model constant. The primary feature of the SFMDF is that the chemical source terms (S_α) appear in closed form.

2.4 FDF SIMULATION

The FDF transport equation is solved via a Lagrangian Monte Carlo (MC) method on a domain portrayed by finite difference (FD) grid points. In this setting, the FDF is represented by an ensemble of MC particles. Each particle is transported in physical space due to convection along with molecular and subgrid diffusion. The composition of these particles change due to mixing and chemical reaction. The spatial transport is represented by the general diffusion process, described by the stochastic differential equation (SDE) [154, 155]:

$$\mathrm{d}X_i(t) = D_i\left(\mathbf{X}(t), t\right)\mathrm{d}t + E\left(\mathbf{X}(t), t\right)\mathrm{d}W_i(t), \tag{2.21}$$

where X_i denotes the Lagrangian position of a MC particle, $W_i(t)$ is the Wiener-Levy process [156], D_i the "drift" coefficient and E the "diffusion" coefficient. These are determined by comparing the Fokker-Planck corresponding to Eq. (2.21) with the spatial derivatives of Eq. (2.20):

$$\mathrm{d}X_i^+ = \left[\left\langle u_i\right\rangle_L + \frac{1}{\left\langle\rho\right\rangle_\ell}\frac{\partial(\gamma+\gamma_t)}{\partial x_i}\right]\mathrm{d}t + \sqrt{2\left(\gamma+\gamma_t\right)/\left\langle\rho\right\rangle_\ell}\,\mathrm{d}W_i. \tag{2.22}$$

The compositional changes are governed by:

$$\frac{\mathrm{d}\phi_\alpha^+}{\mathrm{d}t} = -\Omega_m\left(\phi_\alpha^+ - \left\langle\phi_\alpha\right\rangle_L\right) + S_\alpha(\boldsymbol{\phi}^+), \tag{2.23}$$

where $\phi_\alpha^+ = \phi_\alpha^+(\mathbf{X}(t), t)$ denotes a scalar value of a MC particle having the Lagrangian position $\mathbf{X}$. By the principle of *equivalent systems* [36, 157], the solutions of Eqs. (2.22) and (2.23) provide the same statistics as the direct solution of the modeled SFMDF transport equation. The numerical integration of Eq. (2.22) is via the Euler-Maruyama approximation [157]:

$$X_i^+\left(t_{k+1}\right) = X_i^+\left(t_k\right) + D_i^+\left(t_k\right)\Delta t + E^+\left(t_k\right)\left(\Delta t\right)^{1/2}\xi_i^+\left(t_k\right), \tag{2.24}$$

where $\Delta t = t_{k+1} - t_k$, ξ_i^+ represents a random variable having a normal distribution, and D_i^+ and E^+ represent the drift and diffusion coefficients evaluated at the particle position $X_i^+\left(t_k\right)$.

The MC algorithm is coupled with the explicit MacCormack FD scheme [158] extended for fourth-order accuracy in space by Gottlieb and Turkel [159] for the solution of Eqs.

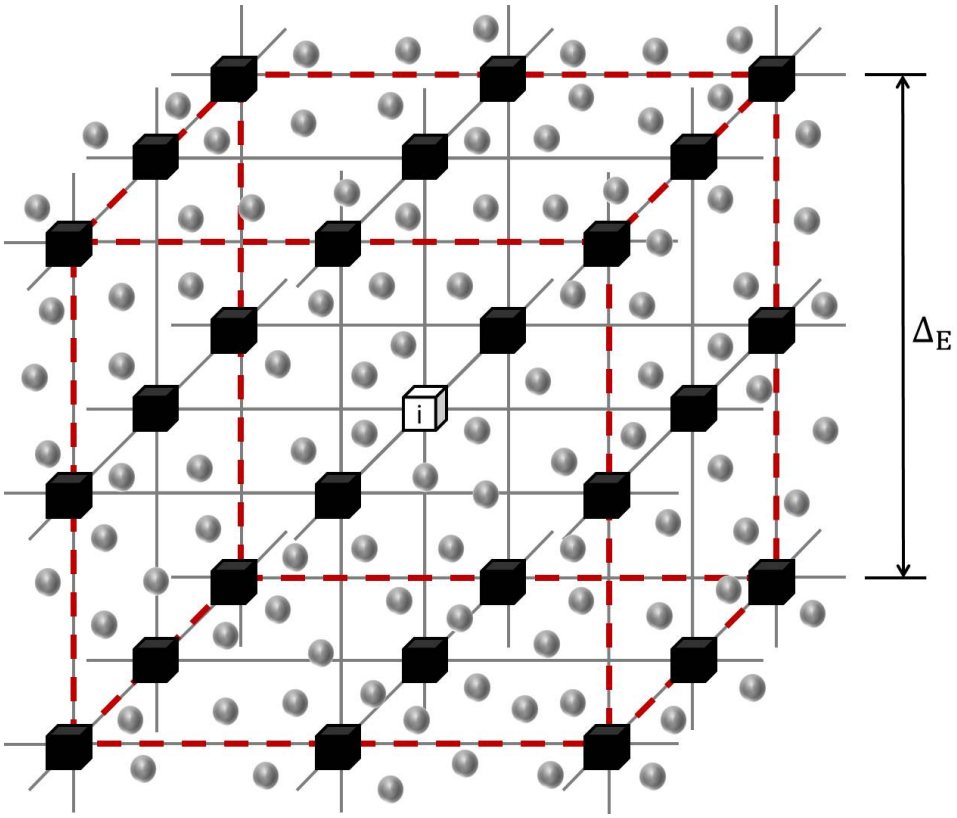

Figure 1: Typical three-dimensional section of the domain in the hybrid simulation. Solid cubes denote FD points. Spheres denote MC particles. The dashed line represents the ensemble domain.

(2.9–2.12). A typical three-dimensional section of the domain is presented in Fig. 1. The communication between the two constituents of this hybrid solver is through interpolation and ensemble averaging. The former is done via simple interpolation of FD values to the particle positions and the latter is by consideration of an ensemble of N_E particles in a domain of size Δ_E^3. This strong coupling of the two solvers makes parallel simulation very challenging. The number of MC particles required for accurate statistics is usually an order of magnitude larger than the number of FD points. For each of these particles, the chemical source terms must be evaluated. In hydrocarbon combustion, this involves a stiff set of coupled nonlinear ordinary differential equations (ODEs). Even with reduced kinetics models and moderate Reynolds numbers, serial simulations would require years of computation [13].

2.5 IPLMCFD

In parallel simulations, the domain is typically divided into an ensemble of subdomains, each assigned to a processor and each containing the same number of FD points and MC particles. This decomposition is done *a priori* and usually remains fixed in time (Fig. 2(a)). In addition to its rather trivial geometrical edge-cut, in such a decomposition, the communications between the neighboring elements is kept to a minimum. However, it exhibits very poor load balancing in dealing with chemistry simulations with finite-rate kinetics. As demonstrated in Fig. 2(b), due to the local nature of chemical reactions, calculations on a few processors continue while the others remain idle. Regions of high computational cost, as presented in Fig. 3, correspond to high reaction zones. For compositions in the cold regions, $S_\alpha \approx 0$; so integration of Eq. (2.23) can be performed over a few implicit sub-steps. In the reacting regions of the flow, this system may be stiff and many implicit sub-steps may be required. The total walltime each subdomain spends on integration will, therefore, be quite disparate for uniform decompositions.

A variety of methodologies have been developed to deal with the computationally expensive turbulent combustion simulation. For a flame near equilibrium, the *flamelet* approximation has been useful [160]. In this approach, the thermochemical variables are related to the

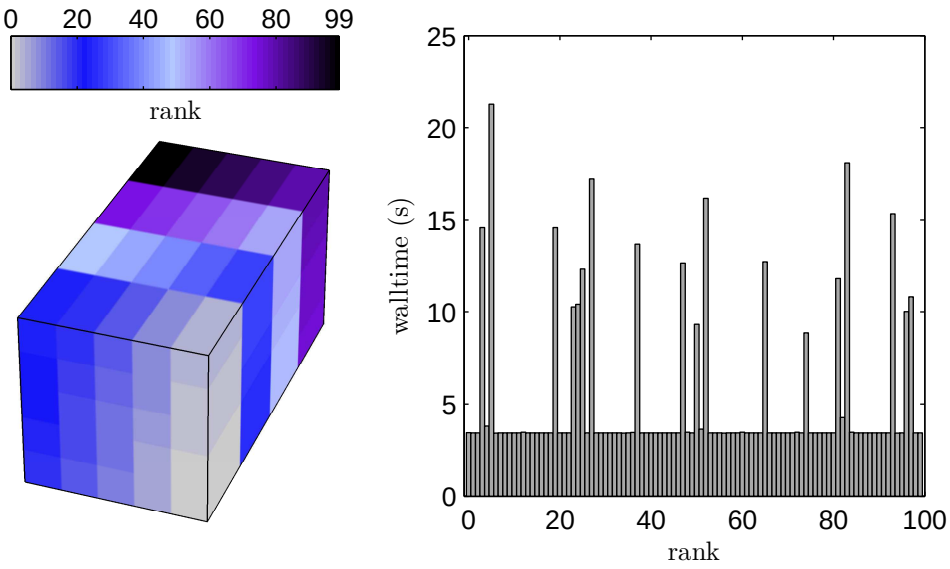

(a) (b)

Figure 2: (**a**) Subdomain boundaries and (**b**) walltime per timestep for each subdomain for the uniform decomposition.

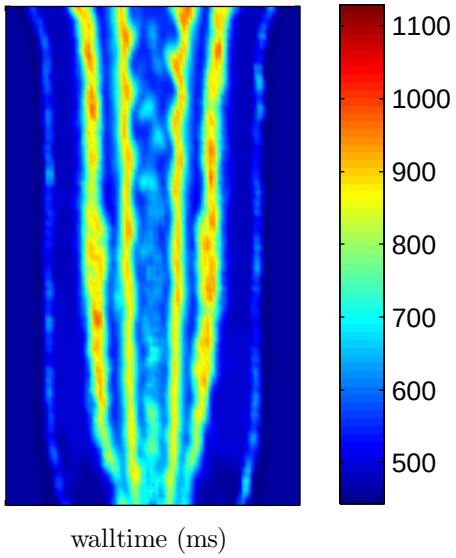

Figure 3: Instantaneous CPU time in milliseconds spent performing particle integration.

mixture fraction, which is a passive scalar variable. This approach reduces the computation time dramatically. The *in situ* adaptive tabulation (ISAT) approach [161–166] is another powerful method which combines table lookup with direct integration to allow treatment of a broad range of reacting flows. ISAT is based on the concept that many particle compositions of the flow are similar and reappear repeatedly throughout the simulation. Thus direct integration is conducted once for a given composition and is stored in a table. If a particle's composition resides in the table, the lookup combined with interpolation is performed in lieu of direct integration. This results in a significant reduction of the total computation time [161]. In theory, the limit of optimal performance would be near that of the flamelet model. In practice, direct integration for a portion of the particles are required for each iteration, resulting in a spatial load imbalance.

In the context of parallel simulation, the *master-slave* strategy is commonly employed to resolve the spatial load imbalance problem. See, for example, Ref. [167]. In this strategy, one process (the master) is in charge of assigning and distributing work to the rest (the slaves). A scalable parallel implementation relies on the ability of the master process to efficiently manage the distribution. Obviously, this becomes increasingly difficult as the number of slave processes increases.

The scheme developed here is termed "irregularly portioned Lagrangian Monte Carlo finite difference" (IPLMCFD). In this scheme, the computational domain is decomposed into irregularly shaped subdomains. Each subdomain is an entirely self-contained hybrid Eulerian/Lagrangian flow solver. The communication between the Lagrangian and Eulerian solvers is purely local, and the shared information among subdomains, typical of FD and MC methods, is limited to neighbors only. This shared information, corresponding to data that is calculated on neighboring subdomains but required locally, is stored in extra elements of each local data array commonly referred to as *ghost points* [168]. For the FD solver, these ghost points correspond to the stencils used for differentiation. For the MC solver, they correspond to the cloud of cells surrounding a given cell, required for interpolation and ensemble averaging as discussed in §2.4. All communication among subdomains is via the Message-Passing Interface (MPI) [168]. As outlined in [167], when utilizing more processors for a fixed problem size, the subdomains become smaller and the ratio of ghost points to

local data points increases. At some stage the communication overhead becomes significant relative to the local computation, and the scalability begins to tail off.

An even distribution of the CPU load is the primary factor in determining the shape of the subdomains. The CPU time, as depicted in Fig. 3, is fed into a weighted graph partitioning algorithm [169]. This algorithm decomposes the domain such that each subdomain is responsible for the same amount of work in terms of CPU time. Simultaneously, it aims to minimize the edge-cuts of each subdomain. A resulting decomposition is presented in Fig. 4(a). The downside to such a decomposition is that the resulting communication among neighboring subdomains can be quite arbitrary and requires significant bookkeeping. However, the major advantage is that the computational load is efficiently balanced, as shown in Fig. 4(b). Further, since each subdomain is a self-contained hybrid solver, it is trivial to include other cost reducing chemistry solvers, such as ISAT, *etc.*

The cost of re-balancing the load is characterized by the necessary amount of data migration between the two decompositions. The spatial distribution of the computational load depends on the physics of the problem and varies in a transient manner. Ideally, if the cost of domain decomposition and re-decomposition are zero, each iteration would begin with a perfectly balanced load. Qualitatively, this temporal deterioration of load balance is case dependent. An example of the temporal performance of the domain decomposition is presented in §2.6.1.

2.6 RESULTS

2.6.1 Scalability

The computational efficiency of the IPLMCFD methodology is examined here by its application for LES of a premixed Bunsen burner flame [170]. This flame consists of a main jet ($D = 12$ mm) having a stoichiometric mixture of methane (CH_4) and air. The Reynolds number of the jet is $22,400$. These simulations are conducted with 2.5×10^6 FD points and 2×10^7 MC particles on Kraken, which is a Cray XT5 system with the National Institute

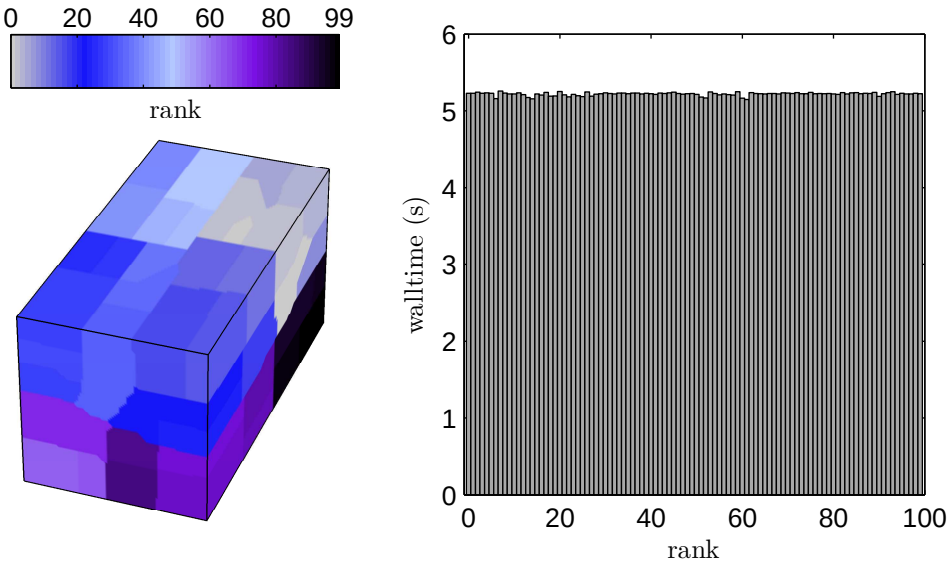

(a) (b)

Figure 4: (**a**) Subdomain boundaries and (**b**) walltime per timestep for each subdomain for the IPLMCFD methodology.

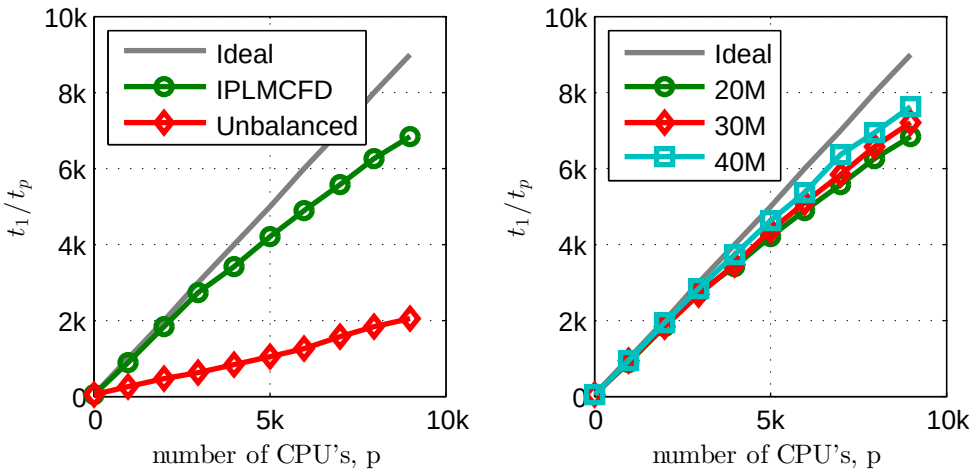

Figure 5: (**a**) Strong scaling comparisons of the IPLMCFD vs. an unbalanced decomposition. (**b**) Strong scaling of the IPLMCFD for an increasing number of MC particles.

for Computational Sciences (NICS). It features 9,048 nodes, with 12 cores per node. Combustion chemistry is described by the reduced mechanism of Mallampalli *et al.* [171], which involves nine species and five reaction steps.

The strong scaling (or speed-up) of the IPLMCFD methodology is compared to that of the uniform decomposition in Fig. 5(a). This scaling, is defined as the ratio of sequential walltime (t_1) to the walltime using p processors (t_p). The timing is averaged over ten iterations immediately after load balancing. Up to a few thousand processors, the IPLMCFD methodology is nearly ideally efficient offering a tremendous improvement over the uniform decomposition. Comparatively, with 2,000 processors the efficiency is 92%; whereas, that of the unbalanced decomposition is only 21%. At 8,000 processors, the IPLMCFD is still performing with an efficiency of around 75%, which is very favorable considering the relatively small size of the test geometry.

To obtain more accurate statistics from the Lagrangian solver, it is necessary to increase the amount of MC particles in each ensemble domain. Figure 5(b) indicates that as the number of MC particles increases, the strong scaling of the IPLMCFD methodology improves.

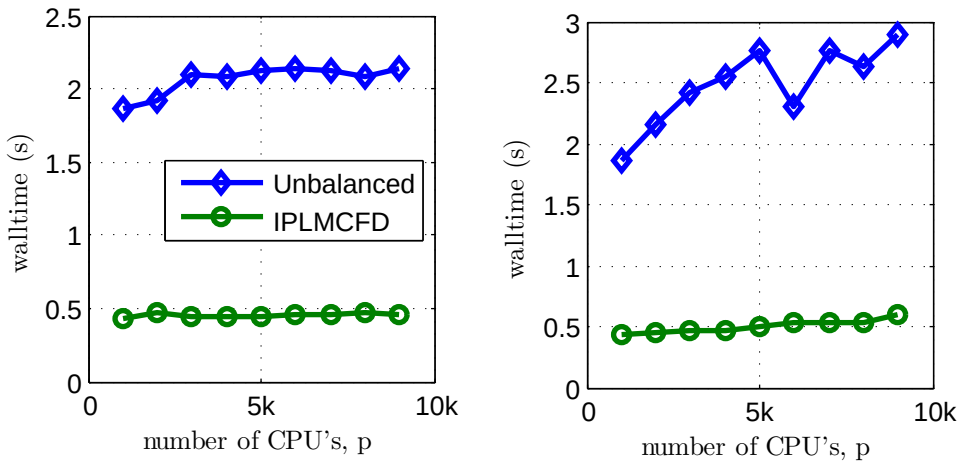

(a) (b)

Figure 6: (**a**) Weak scaling comparisons of the IPLMCFD vs. an unbalanced decomposition for a fixed ratio of cells per processor. (**b**) Weak scaling of the IPLMCFD for a fixed ratio of MC particles per processor.

While using more MC particles necessarily costs more in terms of overall walltime, this increase comes at a substantial discount due to the increased overall efficiency.

The weak scaling of the IPLMCFD is presented in Figs. 6(a) and 6(b). By adding cells to the computational domain (to increase its size, for example), the walltime ideally should remain constant as the number of processors is proportionally increased. This is indeed the case as shown in Fig. 6(a) in which the ratio of the number of cells to the number of processors is held fixed. The *unbalanced* case corresponds to a decomposition with a uniform weight graph partition. In Fig. 6(b) the ratio of the number of MC particles to the number of processors is held fixed. Again the IPLMCFD exhibits an excellent performance.

The temporal performance of the IPLMCFD is quantified in Fig. 7. For this case, $2,048$ processors are employed, and load balancing is performed every $2,000$ iterations. It is shown that the unbalanced decomposition has a static performance, as the simulation marches in time. Immediately after load balancing the IPLMCFD operates at its optimal performance. This may slowly degrade as the simulation proceeds, until the next load balancing operation.

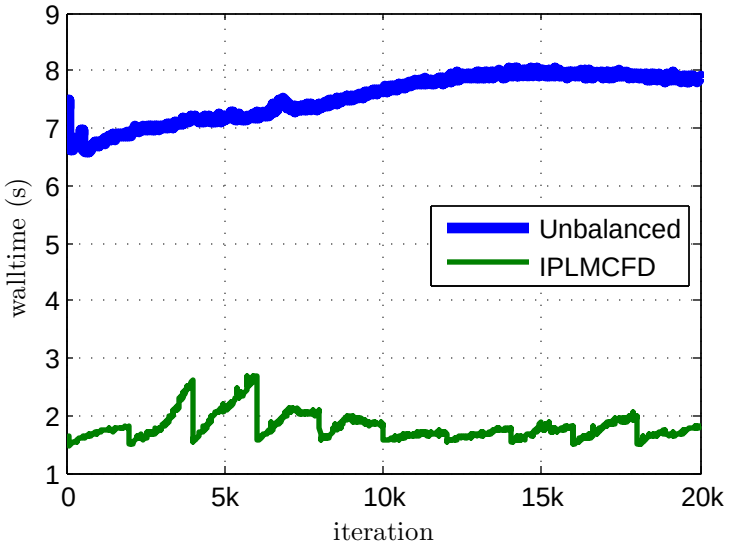

Figure 7: Performance in time of the IPLMCFD vs. an unbalanced decomposition.

The degradation is most pronounced initially, as the solver sweeps the initial condition out of the domain. The integral of the difference between the *unbalanced* case and IPLMCFD over the number of iterations provides the measure of the total walltime savings afforded by the IPLMCFD (excluding the cost of re-decomposition).

2.6.2 Realizability

The realizability of the IPLMCFD solver is assessed by LES of a turbulent jet flow under the influence of an exothermic chemical reaction $\mathcal{A} + \mathcal{B} \longrightarrow \mathcal{P} + \text{Heat}$. The rate of reactant conversion is governed by $S_{\text{A}} = -\rho k \text{AB}$, where A and B are the mass fractions of species $\mathcal{A}$ and $\mathcal{B}$. The jet has a fuel composition of $\text{A}_\infty = 1$ and temperature $T_A = 300$ K. The coflow has oxidizer composition of $\text{B}_\infty = 1$ and temperature $T_B = 300$ K. The heat release, $Q/C_p = 1,400$ K; yielding the adiabatic flame temperature of $1,000$ K. To assess realizability, the scalar values along with the temperature are presented in the domain of the mixture fraction. Here the mixture fraction, ξ, is defined such that $\xi = 1$ in the fuel stream, $\xi = 0$ in the oxidizer stream and $\xi = 0.5$ on the flame surface.

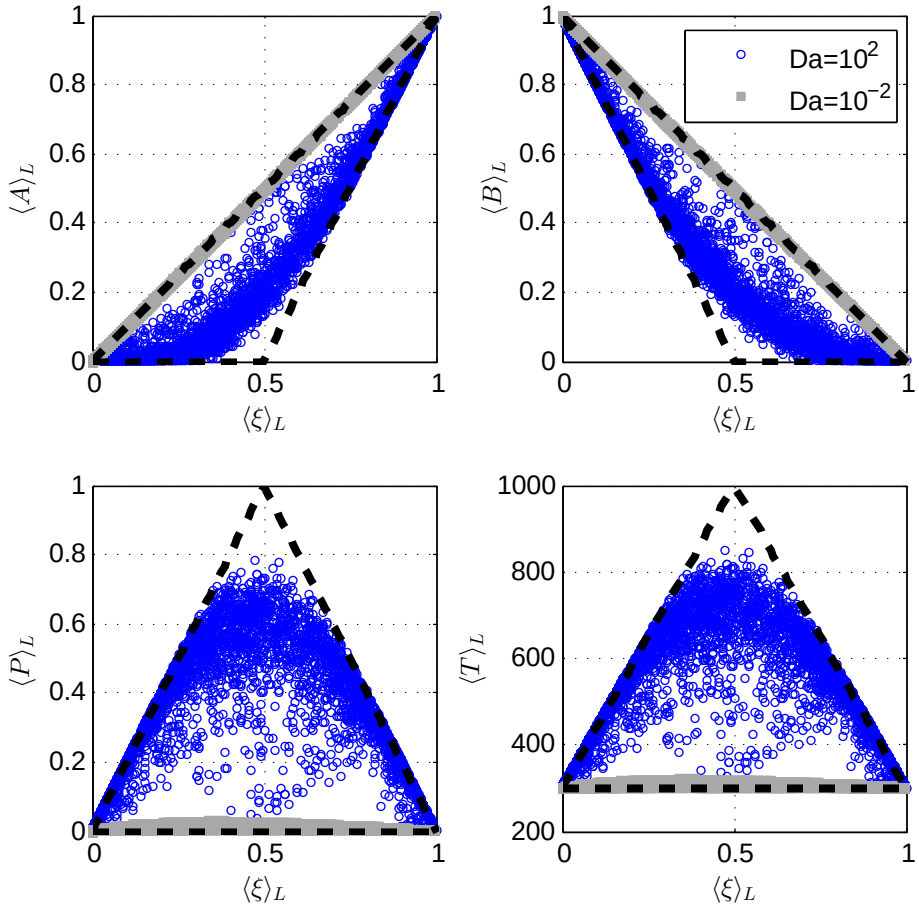

Figure 8: Scatter plots of the filtered composition variables vs. the filtered mixture fraction for $Da = 10^{-2}$ and $Da = 10^{2}$. The dashed lines denote pure mixing and infinitely fast chemistry limits.

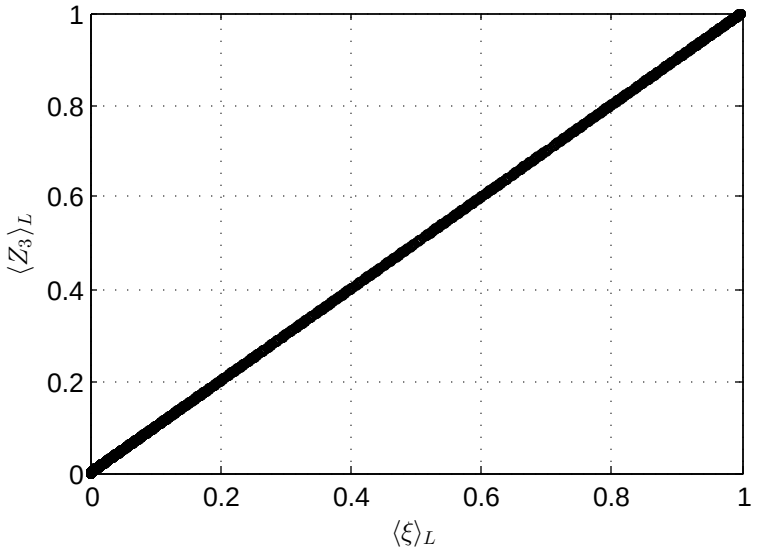

Figure 9: Scatter plot comparing Z_3 vs. the mixture fraction for $Da = 10^2$.

The reaction rate (k) is parameterized in terms of the Damköhler number, $Da = \frac{\rho_0 L_0 k}{u_0}$, where ρ_0, L_0 and u_0 represent a reference density, length and velocity respectively. As shown in Fig. 8, two cases are considered: a (relatively) slow reaction rate ($Da = 10^{-2}$) and a fast rate ($Da = 10^2$). For the former, the composition is close to that of pure mixing. For the latter, the composition is close to that of infinitely fast reaction. For other finite values of Da, the realizable region include the states between the pure mixing and infinitely fast chemistry limits [44].

Transport of three Shvab-Zeldovich conserved scalars are also considered [43, 44]:

$$Z_1 = \frac{\mathrm{A} + \frac{\mathrm{P}}{r+1}}{\mathrm{A}_\infty}, \quad Z_2 = \frac{\mathrm{B} + \frac{r\mathrm{P}}{r+1} - \mathrm{B}_\infty}{-\mathrm{B}_\infty}, \quad Z_3 = \frac{\frac{C_p}{Q}(T - T_B) + \mathrm{A}}{\frac{C_p}{Q}(T_A - T_B) + \mathrm{A}_\infty} \tag{2.25}$$

The consistency of a conserved scalar with the mixture fraction is shown to be nearly perfectly correlated in Fig. 9 for the case when $Da = 10^2$. The results for the case of $Da = 10^{-2}$ and the other conserved scalars are similar; thus are not presented.

2.6.3 Consistency and Reliability

To demonstrate the predictive capability of the IPLMCFD methodology, sample results are presented for the simulation of a turbulent nonpremixed piloted flame. Sandia Flame D [172–174] is considered for this purpose. This flame consists of a main fuel jet ($D = 7.2$ mm) composed of a mixture of 25% methane (CH_4) and 75% air by volume at a temperature of 294 K. The jet has a bulk velocity of 49.6 m/s and a Reynolds number of $22,400$. The fuel jet is surrounded by a lean pilot mixture of C_2H_2, H_2, air, CO_2 and N_2 at $1,880$ K. The measured axial velocity of the pilot gases at the burner exit is 11.4 m/s. The jet and pilot are surrounded by a coflow of air at 291 K with an axial velocity of 0.9 m/s. A schematic of the burner is presented in Fig. 10.

The simulation was conducted on a uniformly spaced, three-dimensional Cartesian mesh. The number of grid points in each coordinate direction is $101 \times 101 \times 101$, mapping to a physical space of size $20D \times 10D \times 10D$. An odd number of grid points is used to ensure that a point lies along the centerline of jet. The filter size is set as $\Delta_G = 2\left(\Delta x \Delta y \Delta z\right)^{1/3}$, where Δx, Δy and Δz are the grid spacing in each coordinate direction. The model parameters used are given in Table 1.

To describe the chemistry, finite-rate kinetics are employed via the augmented reduced mechanism of Sung *et al.* [175]. This mechanism was developed for methane oxidation from GRI-Mech 1.2 [176, 177]. It features 16 species and 12 lumped reaction steps which are presented in Table 2. The inlet boundary conditions corresponding to the thermochemistry are adapted from Xu and Pope [178] and are presented in Table 3.

Due to the hybrid nature of the IPLMCFD methodology, some of the thermochemical transport variables are available from both the Eulerian and Lagrangian solvers. This redundancy is very useful to examine the solvers' consistency. Figure 11(a) shows the instantaneous contour plots of the filtered mixture fraction as obtained by both solvers. As shown in Fig. 11(b), the consistency is convincing.

For the purpose of flow visualization, Fig. 12 presents isosurfaces of the mixture fraction, temperature and mass fraction of carbon dioxide. Highlighted in this figure are coherent structures, and the relationship among some of the thermochemical variables of interest.

In Figs. 13 - 16 flow statistics are compared with experimental data. These statistics are generated by long-time averaging the instantaneous values of various thermochemical flow variables. The initial condition is allowed to sweep through the computational domain before statistics are collected. In this way, approximately $45,000$ samples were collected. In the referenced figures $\overline{\langle Q \rangle}_L$ denotes the time averaged mean of the Favre filtered variable Q. In general, the agreement with experimental data is excellent. In Fig. 16 there is a modest over-prediction of the temperature as compared to the experiment. This correlates with the profiles of methane and oxygen (Fig. 15) which are under-predicted at the same location. Thus, the simulation is predicting more complete combustion at this location. This observation agrees with the profile of carbon monoxide, a product gas of hydrocarbon combustion, which is shown to be over-predicted at the same location.

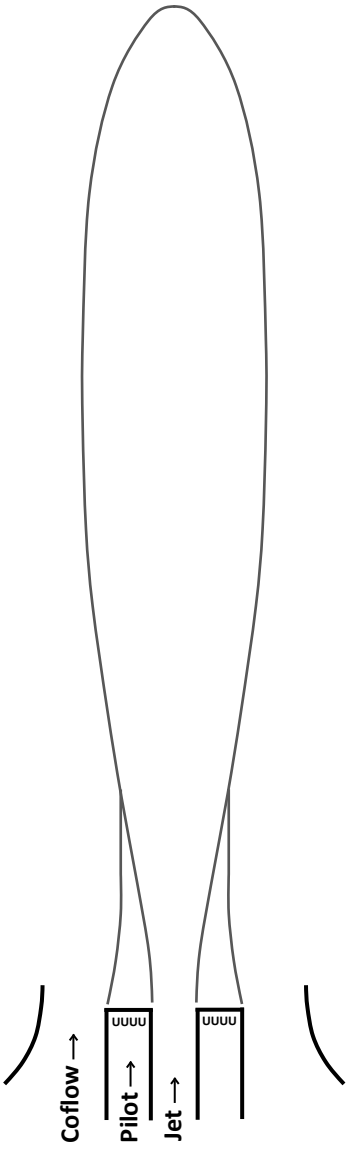

Figure 10: Sandia Flame D burner configuration.

Table 1: Sandia Flame D simulation model parameters.

Parameter	Description	Value
C_R	MKEV model constant	0.02
C_I	MKEV model constant	0.00
$\mathcal{U}_1$	MKEV x-dir. reference velocity	32.0 m/s
$\mathcal{U}_2$	MKEV y-dir. reference velocity	0.00 m/s
$\mathcal{U}_3$	MKEV z-dir. reference velocity	0.00 m/s
C_Ω	LMSE model constant	8.00
Sc	Schmidt number	0.75
Sc_t	SGS Schmidt number	0.75

Table 2: ARM reaction steps and species.

Step	Reaction
1	$O_2 + 2CO = 2CO_2$
2	$H + O_2 + CO = OH + CO_2$
3	$H_2 + O_2 + CO = H + OH + CO_2$
4	$HO_2 + CO = OH + CO_2$
5	$O_2 + H_2O_2 + CO = OH + HO_2 + CO_2$
6	$O_2 + \frac{1}{2}C_2H_2 = H + CO_2$
7	$O_2 + CH_3 + CO + C_2H_4 = CH_4 + CO_2 + CH_2O + \frac{1}{2}C_2H_2$
8	$O_2 + 2CH_3 = H_2 + CH_4 + CO_2$
9	$O_2 + 2CH_3 + CO = CH_4 + CO_2 + CH_2O$
10	$O_2 + CH_3 + CO = H + CO_2 + CH_2O$
11	$O_2 + CO + C_2H_6 = CH_4 + CO_2 + CH_2O$
12	$H + OH = H_2O$

Table 3: Sandia Flame D simulation thermochemistry inlet boundary conditions.

Variable	Coflow	Pilot	Jet
T (K)	291	1880	294
p (atm)	0.993	0.993	0.993
ξ	0.00	0.270	1.00
$Y_{\mathrm{H_2}}$	0.00	$1.29E-4$	0.00
Y_{H}	0.00	$2.52E-5$	0.00
$Y_{\mathrm{O_2}}$	0.231	$5.44E-2$	0.196
Y_{OH}	0.00	$2.81E-3$	0.00
$Y_{\mathrm{H_2O}}$	$6.00E-3$	$9.42E-2$	0.00
$Y_{\mathrm{HO_2}}$	0.00	0.00	0.00
$Y_{\mathrm{H_2O_2}}$	0.00	0.00	0.00
$Y_{\mathrm{CH_3}}$	0.00	0.00	0.00
$Y_{\mathrm{CH_4}}$	0.00	0.00	0.156
Y_{CO}	0.00	$4.06E-3$	0.00
$Y_{\mathrm{CO_2}}$	0.00	0.110	0.00
$Y_{\mathrm{CH_2O}}$	0.00	0.00	0.00
$Y_{\mathrm{C_2H_2}}$	0.00	0.00	0.00
$Y_{\mathrm{C_2H_4}}$	0.00	0.00	0.00
$Y_{\mathrm{C_2H_6}}$	0.00	0.00	0.00
$Y_{\mathrm{N_2}}$	0.763	0.735	0.647

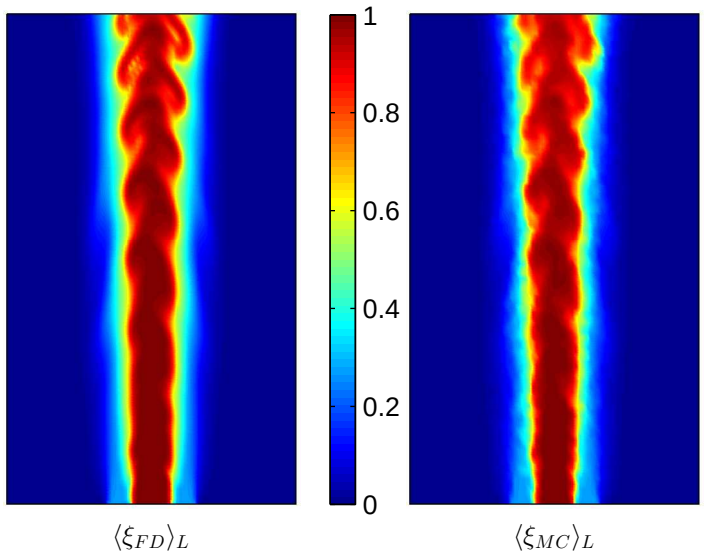

(a)

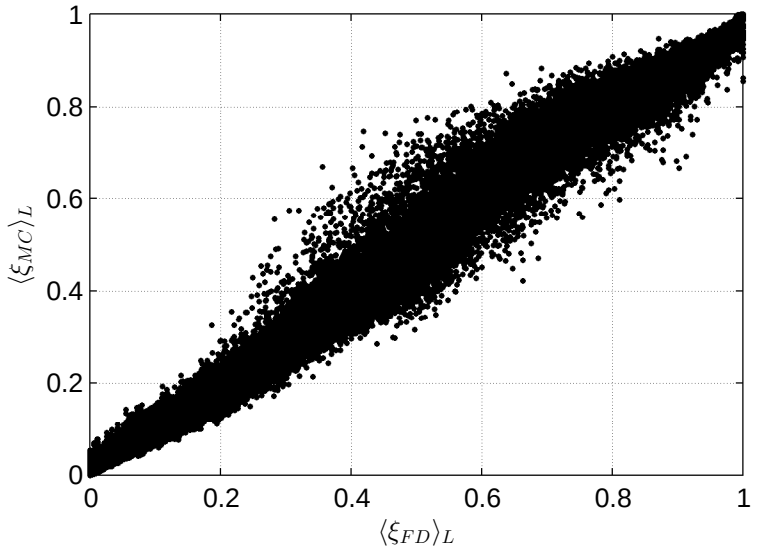

(b)

Figure 11: Comparison of the mixture fraction as calculated by the FD solver and the MC solver. (**a**) Visual comparison of a slice of the domain. (**b**) Scatter plot comparing the entire domain.

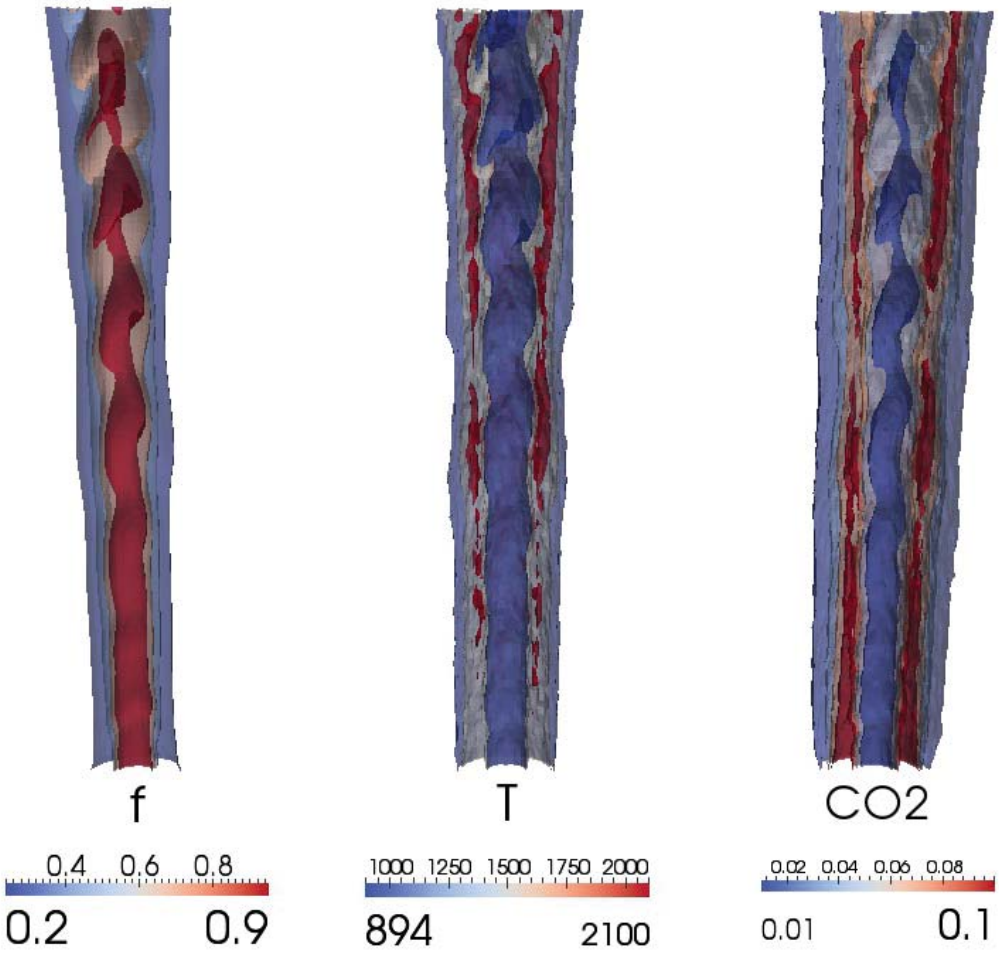

Figure 12: Isosurfaces of the mixture fraction, temperature and mass fraction of CO_2.

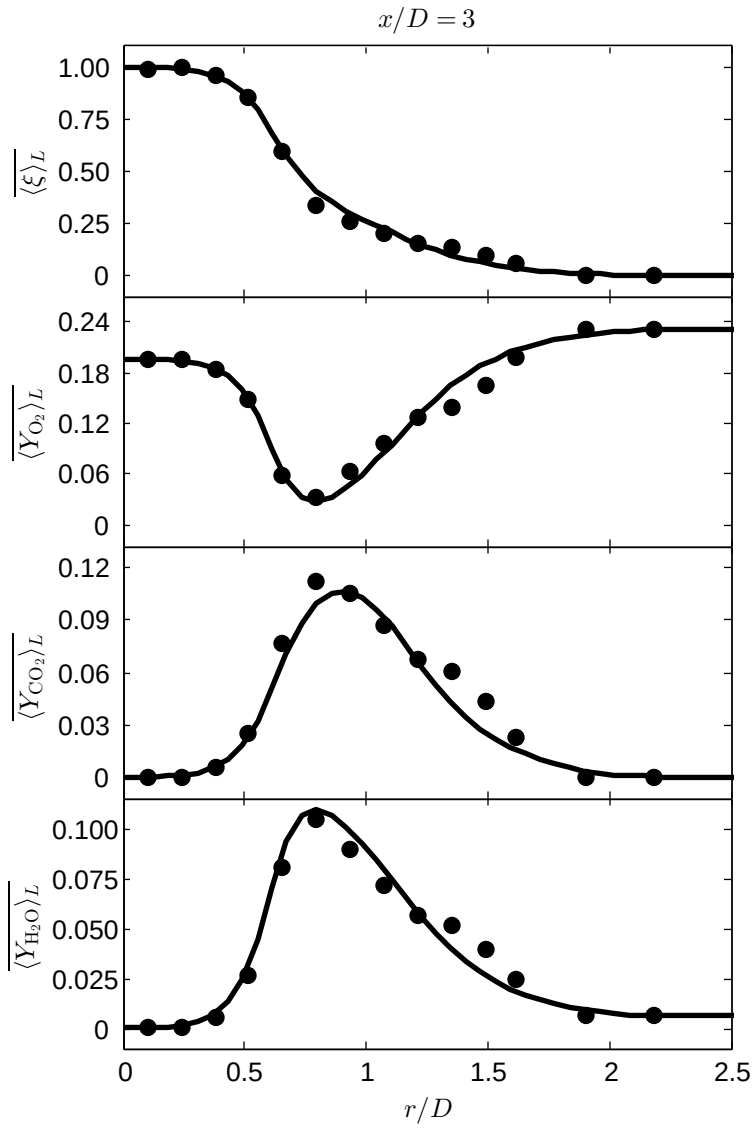

Figure 13: Radial profiles of the mean mixture fraction and the mean O_2, CO_2 and H_2O mass fractions at $x/D = 3$. —IPLMCFD, ● Experiment.

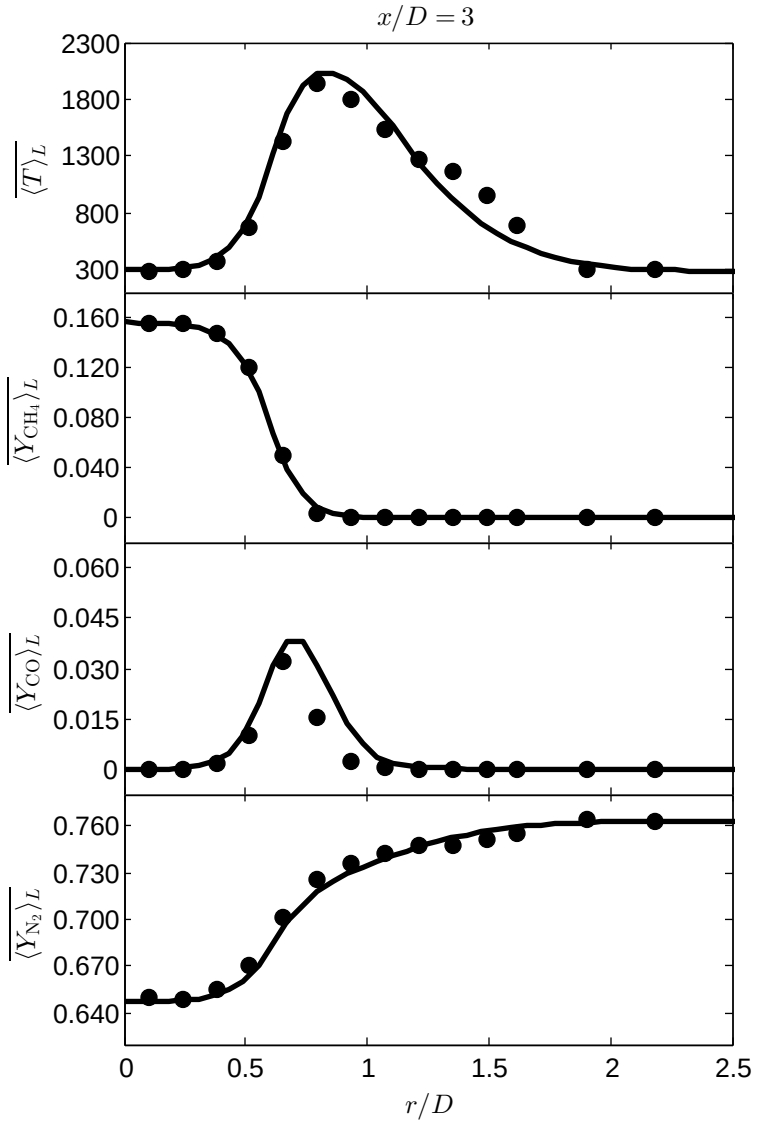

Figure 14: Radial profiles of the mean temperature and the mean CH_4, CO and N_2 mass fractions at $x/D = 3$. —IPLMCFD, ● Experiment.

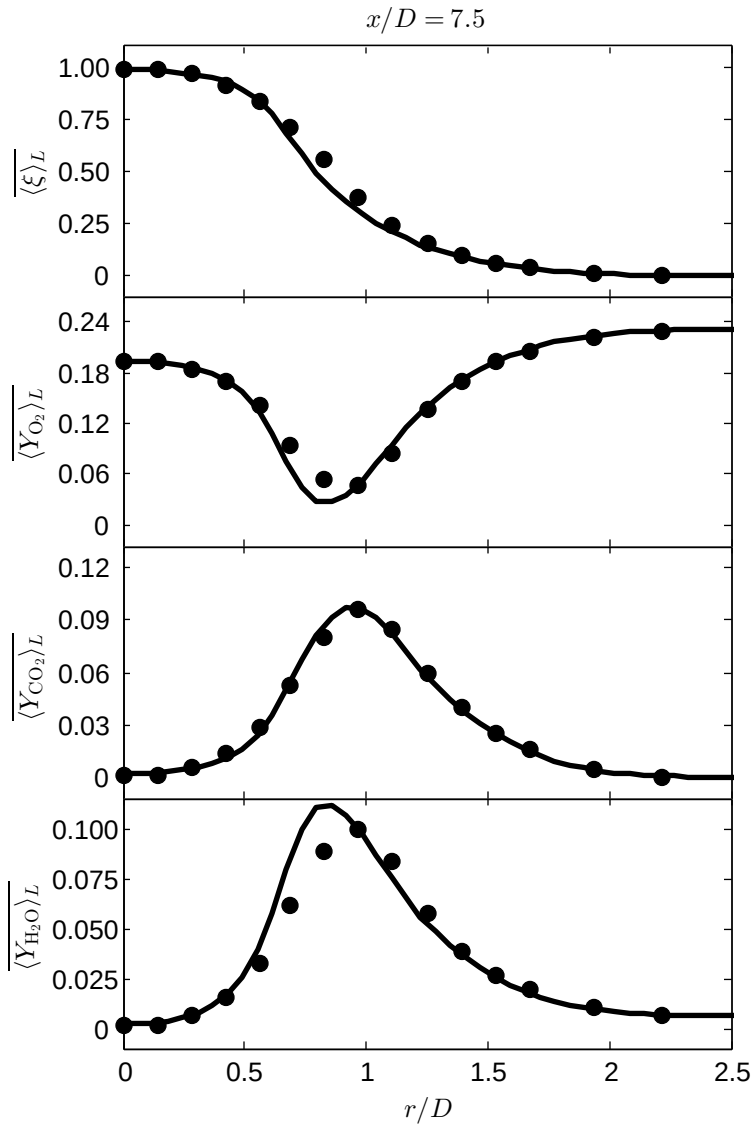

Figure 15: Radial profiles of the mean mixture fraction and the mean O_2, CO_2 and H_2O mass fractions at $x/D = 7.5$. —IPLMCFD, ● Experiment.

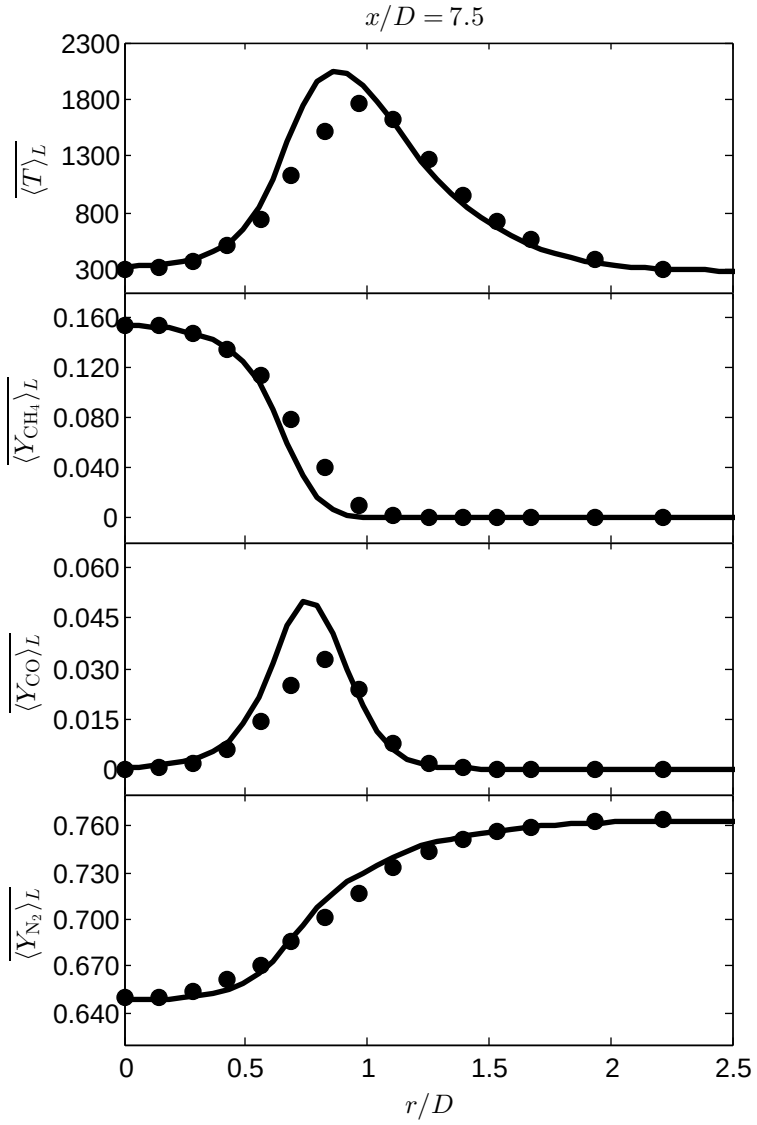

Figure 16: Radial profiles of the mean temperature and the mean CH_4, CO and N_2 mass fractions at $x/D = 7.5$. —IPLMCFD, ● Experiment.

3.0 CONCLUSIONS

The filtered density function (FDF) has proven to be a very powerful and reliable tool for large eddy simulation (LES) of turbulent reacting flows. One of the major obstacles for a widespread usage of FDF is its prohibitive computational cost when dealing with complex chemical kinetics and/or large geometries. In this work, the "irregularly portioned Lagrangian Monte Carlo finite difference" (IPLMCFD) methodology is introduced to mitigate this cost and to take advantage of modern parallel platforms. This methodology addresses the load balancing issue by decomposing the computational domain into a series of irregularly shaped and sized subdomains. The resulting algorithm scales to thousands of processors with an excellent efficiency. The realizability, consistency and the predictive capability of the FDF are assessed by LES of several turbulent reacting flow configurations.

Future work on the IPLMCFD methodology is recommended to be focused on the following areas:

1. Applications to more complex test cases.
2. Incorporation of more advanced FDF models.
3. Development of an efficient load re-balancing procedure.
4. Improvement in scalability through hybrid parallelism.

3.1 FURTHER APPLICATIONS

The IPLMCFD is recommended to be applied for LES of more complex reacting flows. Two particular cases are recommended for immediate applications. The first is a turbulent

lifted hydrogen jet flame in a heated coflow. This case has been the subject of recent direct numerical simulation (DNS) [179]. The flame is auto-ignited and is lifted, thus it provides a good example of partially premixed combustion. The second case is based on the transverse hydrogen jet issuing perpendicularly into a cross-flow of heated air as considered by DNS [180]. The cross-flow is over a wall boundary which will present a challenge for LES. Both cases involve hydrogen fuel, which offers a departure from the hydrocarbon combustion as considered here. Eventually, the methodology can be applied for LES of practical problems [145].

3.2 OTHER FDF CLOSURES

The scalar filtered mass density function (SFMDF), is applicable to low-speed reacting flows. The IPLMCFD can be extended to offer a scalable algorithm for treatment of high-speed flows including hypersonics. This involves establishing a general framework for the inclusion of additional FDF models into IPLMCFD. In doing so, the energy-pressure-velocity-scalar filtered mass density function (EPVS-FMDF) [11, 12] will allow the treatment of high-speed reacting flows. Also, more precise FDF models for low-speed reacting flows, such as the velocity-scalar (VSFMDF) [9] and the frequency-velocity-scalar (FVS-FMDF) [10] can be included as well.

3.3 DYNAMIC PARTITIONING

At present, the partitioning and re-partitioning of the domain into load balanced, irregularly shaped subdomains is performed at user-defined intervals. This is not a highly efficient process as it involves saving the current state of the simulation and restarting with the new decomposition. It is recommended to develop an efficient dynamic load re-balancing procedure which aims to minimize the data migration between the existing decomposition and a new decomposition, and to do so without halting the simulation. This can be achieved through the utilization of existing data management and re-partitioning tools [181, 182].

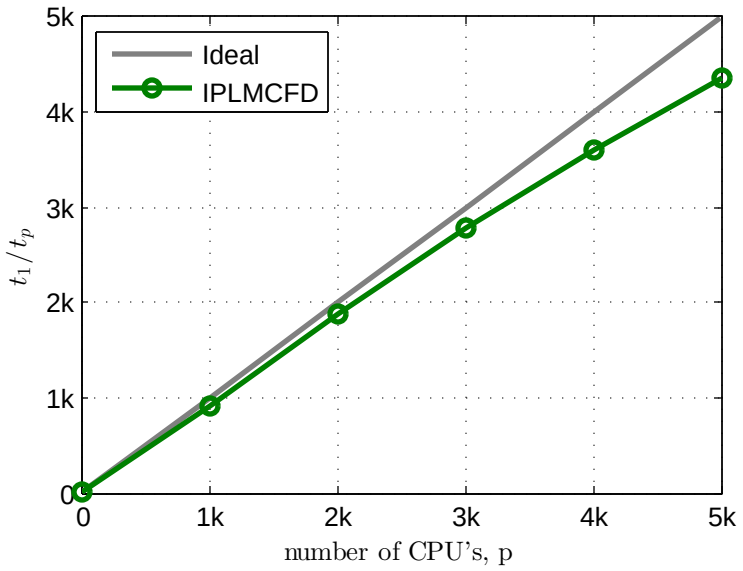

Figure 17: Strong scaling of the IPLMCFD with only one core per a node utilized.

3.4 HYBRID PARALLELISM

A relatively longer term goal is to exploit the multi-core hybrid architecture of the modern supercomputers through hybrid parallelism. In this case, distributed parallelism will be utilized among the nodes via MPI as in the current implementation. While shared parallelism will be utilized among the cores residing on a node via OpenMP [183]. In an effort to assess how the IPLMCFD scales on a purely node based level, the strong scaling analysis of §2.6.1 was repeated utilizing only one core per a node. The results are presented in Fig. 17, and indicate that excellent strong scaling is achieved for distributed parallelism utilizing $5,000$ nodes. These results are from simulations on Kraken, which is a Cray XT5 system with the National Institute for Computational Sciences (NICS) featuring $9,048$ nodes, with 12 cores per node. Thus if all cores per a node can be efficiently utilized via shared parallelism, Fig. 17 indicates that IPLMCFD will scale to $60,000$ cores.

BIBLIOGRAPHY

[1] Givi, P., Filtered Density Function for Subgrid Scale Modeling of Turbulent Combustion, *AIAA J.*, **44**(1):16–23 (2006).

[2] Givi, P., Model-Free Simulations of Turbulent Reactive Flows, *Prog. Energ. Combust.*, **15**(1):1–107 (1989).

[3] Pope, S. B., Computations of Turbulent Combustion: Progress and Challenges, *Proc. Combust. Inst.*, **23**(1):591–612 (1990).

[4] Ansari, N., Jaberi, F. A., Sheikhi, M. R. H., and Givi, P., Filtered Density Function as a Modern CFD Tool, in Maher, A. R. S., editor, *Engineering Applications of Computational Fluid Dynamics: Volume 1*, Chapter 1, pp. 1–22, International Energy and Environment Foundation, 2011.

[5] Colucci, P. J., Jaberi, F. A., Givi, P., and Pope, S. B., Filtered Density Function for Large Eddy Simulation of Turbulent Reacting Flows, *Phys. Fluids*, **10**(2):499–515 (1998).

[6] Jaberi, F. A., Colucci, P. J., James, S., Givi, P., and Pope, S. B., Filtered Mass Density Function for Large-Eddy Simulation of Turbulent Reacting Flows, *J. Fluid Mech.*, **401**:85–121 (1999).

[7] Gicquel, L. Y. M., Givi, P., Jaberi, F. A., and Pope, S. B., Velocity Filtered Density Function for Large Eddy Simulation of Turbulent Flows, *Phys. Fluids*, **14**(3):1196–1213 (2002).

[8] Sheikhi, M. R. H., Drozda, T. G., Givi, P., and Pope, S. B., Velocity-Scalar Filtered Density Function for Large Eddy Simulation of Turbulent Flows, *Phys. Fluids*, **15**(8):2321–2337 (2003).

[9] Sheikhi, M. R. H., Givi, P., and Pope, S. B., Velocity-Scalar Filtered Mass Density Function for Large Eddy Simulation of Turbulent Reacting Flows, *Phys. Fluids*, **19**(9):095106 (2007).

[10] Sheikhi, M. R. H., Givi, P., and Pope, S. B., Frequency-Velocity-Scalar Filtered Mass Density Function for Large Eddy Simulation of Turbulent Flows, *Phys. Fluids*, **21**(7):075102 (2009).

[11] Nik, M. B., Givi, P., Madnia, C. K., and Pope, S. B., EPVS-FMDF for LES of High-Speed Turbulent Flows, in *50th AIAA Aerospace Sciences Meeting including the New Horizons Forum and Aerospace Exposition*, pp. 1–12, Nashville, TN, 2012, AIAA, AIAA-2012-117.

[12] Nik, M. B., VS-FMDF and EPVS-FMDF for Large Eddy Simulation of Turbulent Flows, Ph.D. Thesis, Department of Mechanical Engineering and Materials Science, University of Pittsburgh, Pittsburgh, PA, 2012.

[13] Yilmaz, S. L., Nik, M. B., Sheikhi, M. R. H., Strakey, P. A., and Givi, P., An Irregularly Portioned Lagrangian Monte Carlo Method for Turbulent Flow Simulation, *J. Sci. Comput.*, **47**(1):109–125 (2011).

[14] Pope, S. B., *Turbulent Flows*, Cambridge University Press, Cambridge, U.K., 2000.

[15] Menon, S., Subgrid Combustion Modelling for Large-Eddy Simulations, *Int. J. Engine Res.*, **1**(2):209–227 (2000).

[16] Bilger, R. W., Future Progress in Turbulent Combustion Research, *Prog. Energ. Combust.*, **26**(4–6):367–380 (2000).

[17] Veynante, D. and Vervisch, L., Turbulent Combustion Modeling, *Prog. Energ. Combust.*, **28**(3):193–266 (2002).

[18] Bilger, R. W., Pope, S. B., Bray, K. N. C., and Driscoll, J. F., Paradigms in Turbulent Combustion Research, *Proc. Combust. Inst.*, **30**(1):21–42 (2005).

[19] Pitsch, H., Large-Eddy Simulation of Turbulent Combustion, *Annu. Rev. Fluid Mech.*, **38**:453–482 (2006).

[20] Echekki, T. and Mastorakos, E., editors, *Turbulent Combustion Modeling: Advances, New Trends and Perspectives*, *Fluid Mechanics and Its Applications*, Vol. 95, Springer Netherlands, 2011.

[21] Williams, F. A., Turbulent Combustion, in Buckmaster, J. D., editor, *The Mathematics of Combustion*, Frontiers in Applied Mathematics, SIAM, Philadelphia, PA, 1985.

[22] Peters, N. and Williams, F. A., Liftoff Characteristics of Turbulent Jet Diffusion Flames, *AIAA J.*, **21**(3):423–429 (1983).

[23] Schumann, U., Large Eddy Simulation of Turbulent Diffusion with Chemical Reactions in the Convective Boundary Layer, *Atmos. Environ.*, **23**(8):1713–1726 (1989).

[24] Libby, P. A. and Williams, F. A., editors, *Turbulent Reacting Flows*, *Topics in Applied Physics*, Vol. 44, Springer-Verlag, Heidelberg, 1980.

[25] Brodkey, R. S., editor, *Turbulence in Mixing Operations: Theory and Application to Mixing and Reaction*, Academic Press, New York, NY, 1975.

[26] Hill, J. C., Homogeneous Turbulent Mixing with Chemical Reaction, *Annu. Rev. Fluid Mech.*, **8**:135–161 (1976).

[27] Frankel, S. H., Adumitroaie, V., Madnia, C. K., and Givi, P., Large Eddy Simulations of Turbulent Reacting Flows by Assumed PDF Methods, in Ragab, S. A. and Piomelli, U., editors, *Engineering Applications of Large Eddy Simulations*, pp. 81–101, ASME, FED-Vol. 162, New York, NY, 1993.

[28] Meeder, J. P. and Nieuwstadt, F. T. M., Subgrid-Scale Segregation of Chemically Reactive Species in a Neutral Boundary Layer, in Chollet, J.-P., Voke, P. R., and Kleiser, L., editors, *Direct and Large-Eddy Simulation II*, *ERCOFTAC Series*, Vol. 5, pp. 301–310, Springer Netherlands, 1997.

[29] Tennekes, H. and Lumley, J. L., *A First Course in Turbulence*, MIT Press, Cambridge, MA, 1972.

[30] Hinze, J. O., *Turbulence*, McGraw Hill Book Company, New York, NY, 1975.

[31] Wilcox, D. C., *Turbulence Modeling for CFD*, DCW Industries, Inc., La Cañada, CA, third edition, 2006.

[32] Toor, H. L., Mass Transfer in Dilute Turbulent and Non-Turbulent Systems with Rapid Irreversible Reactions and Equal Diffusivities, *AIChE J.*, **8**(1):70–78 (1962).

[33] Dopazo, C., Non-Isothermal Turbulent Reactive Flows: Stochastic Approaches, Ph.D. Thesis, Department of Mechanical Engineering, State University of New York at Stony Brook, Buffalo, NY, 1973.

[34] Pope, S. B., The Statistical Theory of Turbulent Flames, *Phil. Trans. R. Soc. Lond. A*, **291**(1384):529–568 (1979).

[35] O'Brien, E. E., The Probability Density Function (PDF) Approach to Reacting Turbulent Flows, in Libby, P. and Williams, F., editors, *Turbulent Reacting Flows*, *Topics in Applied Physics*, Vol. 44, Chapter 5, pp. 185–218, Springer Berlin / Heidelberg, 1980.

[36] Pope, S. B., PDF Methods for Turbulent Reactive Flows, *Prog. Energ. Combust.*, **11**(2):119–192 (1985).

[37] Kollmann, W., The PDF Approach to Turbulent Flow, *Theor. Comp. Fluid Dyn.*, **1**(5):249–285 (1990).

[38] Lundgren, T. S., Distribution Functions in the Statistical Theory of Turbulence, *Phys. Fluids*, **10**(5):969–975 (1967).

[39] Lundgren, T. S., Model Equation for Nonhomogeneous Turbulence, *Phys. Fluids*, **12**(3):485–497 (1969).

[40] Madnia, C. K. and Givi, P., Direct Numerical Simulation and Large Eddy Simulation of Reacting Homogeneous Turbulence, in Galperin, B. and Orszag, S. A., editors, *Large Eddy Simulation of Complex Engineering and Geophysical Flows*, Chapter 15, pp. 315–346, Cambridge University Press, Cambridge, England, 1993.

[41] Burke, S. P. and Schumann, T. E. W., Diffusion Flames, *Ind. Eng. Chem.*, **20**(10):998–1004 (1928).

[42] Williams, F. A., Structure of Flamelets in Turbulent Reacting Flows and Influences of Combustion on Turbulence Fields, in Borghi, R. and Murthy, S. N. B., editors, *Turbulent Reactive Flows*, *Lecture Notes in Engineering*, Vol. 40, pp. 195–212, Springer US, 1989.

[43] Bilger, R. W., Turbulent Flows with Nonpremixed Reactants, in Libby, P. and Williams, F., editors, *Turbulent Reacting Flows*, *Topics in Applied Physics*, Vol. 44, Chapter 3, pp. 65–113, Springer Berlin / Heidelberg, 1980.

[44] Poinsot, T. and Veynante, D., *Theoretical and Numerical Combustion*, R. T. Edwards, Inc., Philadelphia, PA, third edition, 2011.

[45] Peters, N., Laminar Diffusion Flamelet Models in Non-Premixed Turbulent Combustion, *Prog. Energ. Combust.*, **10**(3):319–339 (1984).

[46] Cook, A. W., Riley, J. J., and Kosály, G., A Laminar Flamelet Approach to Subgrid-Scale Chemistry in Turbulent Flows, *Combust. Flame*, **109**(3):332–341 (1997).

[47] DesJardin, P. E. and Frankel, S. H., Large Eddy Simulation of a Nonpremixed Reacting Jet: Application and Assessment of Subgrid-Scale Combustion Models, *Phys. Fluids*, **10**(9):2298–2314 (1998).

[48] de Bruyn Kops, S. M., Riley, J. J., Kosály, G., and Cook, A. W., Investigation of Modeling for Non-Premixed Turbulent Combustion, *Flow Turbul. Combust.*, **60**(1):105–122 (1998).

[49] Cook, A. W. and Riley, J. J., Subgrid-Scale Modeling for Turbulent Reacting Flows, *Combust. Flame*, **112**(4):593–606 (1998).

[50] Pitsch, H. and Steiner, H., Large-Eddy Simulation of a Turbulent Piloted Methane/Air Diffusion Flame (Sandia Flame D), *Phys. Fluids*, **12**(10):2541–2554 (2000).

[51] Muradoglu, M., Liu, K., and Pope, S. B., PDF Modeling of a Bluff-Body Stabilized Turbulent Flame, *Combust. Flame*, **132**(1–2):115–137 (2003).

[52] Sheikhi, M. R. H., Drozda, T. G., Givi, P., Jaberi, F. A., and Pope, S. B., Large Eddy Simulation of a Turbulent Nonpremixed Piloted Methane Jet Flame (Sandia Flame D), *Proc. Combust. Inst.*, **30**(1):549–556 (2005).

[53] Drozda, T. G., Sheikhi, M. R. H., Madnia, C. K., and Givi, P., Developments in Formulation and Application of the Filtered Density Function, *Flow Turbul. Combust.*, **78**(1):35–67 (2007).

[54] Nik, M. B., Yilmaz, S. L., Givi, P., Sheikhi, M. R. H., and Pope, S. B., Simulation of Sandia Flame D Using Velocity-Scalar Filtered Density Function, *AIAA J.*, **48**(7):1513–1522 (2010).

[55] Klimenko, A. Y., Multicomponent Diffusion of Various Admixtures in Turbulent Flow, *Fluid Dyn.*, **25**(3):327–334 (1990).

[56] Bilger, R. W., Conditional Moment Closure for Turbulent Reacting Flow, *Phys. Fluids*, **5**(2):436–444 (1993).

[57] Bushe, W. K. and Steiner, H., Conditional Moment Closure for Large Eddy Simulation of Nonpremixed Turbulent Reacting Flows, *Phys. Fluids*, **11**(7):1896–1906 (1999).

[58] Steiner, H. and Bushe, W. K., Large Eddy Simulation of a Turbulent Reacting Jet with Conditional Source-Term Estimation, *Phys. Fluids*, **13**(3):754–759 (2001).

[59] Navarro-Martinez, S., Kronenburg, A., and Di Mare, F., Conditional Moment Closure for Large Eddy Simulations, *Flow Turbul. Combust.*, **75**(1–4):245–274 (2005).

[60] Navarro-Martinez, S. and Kronenburg, A., LES-CMC Simulations of a Turbulent Bluff-Body Flame, *Proc. Combust. Inst.*, **31**(2):1721–1728 (2007).

[61] Navarro-Martinez, S. and Kronenburg, A., LES-CMC Simulations of a Lifted Methane Flame, *Proc. Combust. Inst.*, **32**(1):1509–1516 (2009).

[62] Garmory, A. and Mastorakos, E., Capturing Localised Extinction in Sandia Flame F with LES-CMC, *Proc. Combust. Inst.*, **33**(1):1673–1680 (2011).

[63] Stanković, I., Triantafyllidis, A., Mastorakos, E., Lacor, C., and B.Merci, Simulation of Hydrogen Auto-Ignition in a Turbulent Co-flow of Heated Air with LES and CMC Approach, *Flow Turbul. Combust.*, **86**(3–4):689–710 (2011).

[64] Stanković, I., Mastorakos, E., and Merci, B., LES-CMC Simulations of Different Auto-Ignition Regimes of Hydrogen in a Hot Turbulent Air Co-flow, *Flow Turbul. Combust.*, **90**(3):583–604 (2013).

[65] Siwaborworn, P. and Kronenburg, A., Conservative Implementation of LES-CMC for Turbulent Jet Flames, in Nagel, W. E., Kröner, D. H., and Resch, M. M., editors, *High Performance Computing in Science and Engineering '12*, pp. 159–173, Springer Berlin Heidelberg, 2013.

[66] Klimenko, A. Y. and Pope, S. B., The Modeling of Turbulent Reactive Flows Based on Multiple Mapping Conditioning, *Phys. Fluids*, **15**(7):1907–1925 (2003).

[67] Cook, A. W. and Riley, J. J., A Subgrid Model for Equilibrium Chemistry in Turbulent Flows, *Phys. Fluids*, **6**(8):2868–2870 (1994).

[68] Jiménez, J., Liñán, A., Rogers, M. M., and Higuera, F. J., *A priori* Testing of Subgrid Models for Chemically Reacting Non-Premixed Turbulent Shear Flows, *J. Fluid Mech.*, **349**:149–171 (1997).

[69] Wall, C., Boersma, B. J., and Moin, P., An Evaluation of the Assumed Beta Probability Density Function Subgrid-Scale Model for Large Eddy Simulation of Nonpremixed, Turbulent Combustion with Heat Release, *Phys. Fluids*, **12**(10):2522–2529 (2000).

[70] Johnson, N. L., Systems of Frequency Curves Generated by Methods of Translation, *Biometrika*, **36**:149–176 (1949).

[71] Pierce, C. D. and Moin, P., Progress-Variable Approach for Large-Eddy Simulation of Non-Premixed Turbulent Combustion, *J. Fluid Mech.*, **504**:73–97 (2004).

[72] Mahesh, K., Constantinescu, G., Apte, S., Iaccarino, G., Ham, F., and Moin, P., Large-Eddy Simulation of Reacting Turbulent Flows in Complex Geometries, *J. Appl. Mech.*, **73**(3):374–381 (2005).

[73] You, D., Ham, F., and Moin, P., Large-Eddy Simulation Analysis of Turbulent Combustion in a Gas Turbine Engine Combustor, in *Annual Research Briefs – 2008*, pp. 219–230, Center for Turbulence Research, Stanford, CA, 2008.

[74] Kerstein, A. R., A Linear-Eddy Model of Turbulent Scalar Transport and Mixing, *Combust. Sci. Technol.*, **60**(4–6):391–421 (1988).

[75] Kerstein, A. R., Linear-Eddy Modeling of Turbulent Transport. II: Application to Shear Layer Mixing, *Combust. Flame*, **75**(3–4):397–413 (1989).

[76] Kerstein, A. R., Linear-Eddy Modelling of Turbulent Transport. Part 3. Mixing and Differential Molecular Diffusion in Round Jets, *J. Fluid Mech.*, **216**:411–435 (1990).

[77] Kerstein, A. R., Linear-Eddy Modelling of Turbulent Transport. Part 6. Microstructure of Diffusive Scalar Mixing Fields, *J. Fluid Mech.*, **231**:361–394 (1991).

[78] Kerstein, A. R., Linear-Eddy Modeling of Turbulent Transport. Part 4. Structure of Diffusion Flames, *Combust. Sci. Technol.*, **81**(1–3):75–96 (1992).

[79] McMurtry, P. A., Menon, S., and Kerstein, A. R., A Linear Eddy Sub-Grid Model for Turbulent Reacting Flows: Application to Hydrogen-Air Combustion, *Proc. Combust. Inst.*, **24**(1):271–278 (1992).

[80] Kim, W.-W., Menon, S., and Mongia, H. C., Large-Eddy Simulation of a Gas Turbine Combustor Flow, *Combust. Sci. Technol.*, **143**(1–6):25–62 (1999).

[81] Kerstein, A. R., One-Dimensional Turbulence: Model Formulation and Application to Homogeneous Turbulence, Shear Flows, and Buoyant Stratified Flows, *J. Fluid Mech.*, **392**:277–334 (1999).

[82] Kerstein, A. R., Ashurst, W. T., Wunsch, S., and Nilsen, V., One-Dimensional Turbulence: Vector Formulation and Application to Free Shear Flows, *J. Fluid Mech.*, **447**:85–109 (2001).

[83] Kerstein, A. R., One-Dimensional Turbulence: A New Approach to High-Fidelity Subgrid Closure of Turbulent Flow Simulations, *Comput. Phys. Commun.*, **148**(1):1–16 (2002).

[84] Schmidt, R. C., Kerstein, A. R., Wunsch, S., and Nilsen, V., Near-Wall LES Closure Based on One-Dimensional Turbulence Modeling, *J. Comput. Phys.*, **186**(1):317–355 (2003).

[85] McDermott, R. J., Toward One-Dimensional Turbulence Subgrid Closure for Large-Eddy Simulation, Ph.D. Thesis, Department of Chemical Engineering, University of Utah, Salt Lake City, UT, 2005.

[86] Cao, S. and Echekki, T., A Low-Dimensional Stochastic Closure Model for Combustion Large-Eddy Simulation, *J. Turbul.*, **9**(2):1–35 (2008).

[87] Echekki, T. and Park, J., The LES-ODT Model for Turbulent Premixed Flames, in *48th AIAA Aerospace Sciences Meeting Including the New Horizons Forum and Aerospace Exposition*, Orlando, FL, 2010, AIAA, AIAA-2010-207.

[88] Schmidt, R., Kerstein, A. R., and McDermott, R., ODTLES: A Multi-scale Model for 3D Turbulent Flow Based on One-Dimensional Turbulence Modeling, *Comput. Method Appl. M.*, **199**(13–16):865–880 (2010).

[89] Gonzalez-Juez, E. D., Schmidt, R. C., and Kerstein, A. R., ODTLES Simulations of Wall-bounded Flows, *Phys. Fluids*, **23**(12):125102 (2011).

[90] Park, J. and Echekki, T., LES-ODT Study of Turbulent Premixed Interacting Flames, *Combust. Flame*, **159**(2):609–620 (2012).

[91] Mirgolbabaei, H. and Echekki, T., A Novel Principal Component Analysis-based Acceleration Scheme for LES-ODT: An *a priori* Study, *Combust. Flame*, **160**(5):898–908 (2013).

[92] Spalding, D. B., Mixing and Chemical Reaction in Steady Confined Turbulent Flames, *Proc. Combust. Inst.*, **13**(1):649 – 657 (1971).

[93] Spalding, D. B., Development of the Eddy-Break-Up Model of Turbulent Combustion, *Proc. Combust. Inst.*, **16**(1):1657–1663 (1977).

[94] Fureby, C. and Löfström, C., Large-Eddy Simulations of Bluff Body Stabilized Flames, *Proc. Combust. Inst.*, **25**(1):1257–1264 (1994).

[95] Butler, T. D. and O'Rourke, P. J., A Numerical Method for Two Dimensional Unsteady Reacting Flows, *Proc. Combust. Inst.*, **16**(1):1503–1515 (1977).

[96] Colin, O., Ducros, F., Veynante, D., and Poinsot, T., A Thickened Flame Model for Large Eddy Simulation of Turbulent Premixed Combustion, *Phys. Fluids*, **12**(7):1843–1863 (2000).

[97] Charlette, F., Meneveau, C., and Veynante, D., A Power-law Flame Wrinkling Model for LES of Premixed Turbulent Combustion Part I: Non-dynamic Formulation and Initial Tests, *Combust. Flame*, **131**(1–2):159–180 (2002).

[98] Charlette, F., Meneveau, C., and Veynante, D., A Power-law Flame Wrinkling Model for LES of Premixed Turbulent Combustion Part II: Dynamic Formulation, *Combust. Flame*, **131**(1–2):181–197 (2002).

[99] Boileau, M., Staffelbach, G., Cuenot, B., Poinsot, T., and Bérat, C., LES of an Ignition Sequence in a Gas Turbine Engine, *Combust. Flame*, **154**(1–2):2–22 (2008).

[100] Hernández-Pérez, F. E., Yuen, F. T. C., Groth, C. P. T., and Gülder, Ö. L., LES of a Laboratory-scale Turbulent Premixed Bunsen Flame using FSD, PCM-FPI and Thickened Flame Models, *Proc. Combust. Inst.*, **33**(1):1365–1371 (2011).

[101] Wang, G., Boileau, M., and Veynante, D., Implementation of a Dynamic Thickened Flame Model for Large Eddy Simulations of Turbulent Premixed Combustion, *Combust. Flame*, **158**(11):2199–2213 (2011).

[102] Kuenne, G., Ketelheun, A., and Janicka, J., LES Modeling of Premixed Combustion using a Thickened Flame Approach coupled with FGM Tabulated Chemistry, *Combust. Flame*, **158**(9):1750–1767 (2011).

[103] Kerstein, A. R., Ashurst, W. T., and Williams, F. A., Field Equation for Interface Propagation in an Unsteady Homogeneous Flow Field, *Phys. Rev. A*, **37**(7):2728–2731 (1988).

[104] Im, H. G., Lund, T. S., and Ferziger, J. H., Large Eddy Simulation of Turbulent Front Propagation with Dynamic Subgrid Models, *Phys. Fluids*, **9**(12):3826–3833 (1997).

[105] Pitsch, H. and de Lageneste, L. D., Large-Eddy Simulation of Premixed Turbulent Combustion using a Level-Set Approach, *Proc. Combust. Inst.*, **29**(2):2001–2008 (2002).

[106] Pitsch, H., A Consistent Level Set Formulation for Large-Eddy Simulation of Premixed Turbulent Combustion, *Combust. Flame*, **143**(4):587–598 (2005).

[107] Wang, P. and Bai, X., Large Eddy Simulation of Turbulent Premixed Flames using Level-Set G-Equation, *Proc. Combust. Inst.*, **30**(1):583–591 (2005).

[108] Freitag, M. and Janicka, J., Investigation of a Strongly Swirled Unconfined Premixed Flame using LES, *Proc. Combust. Inst.*, **31**(1):1477–1485 (2007).

[109] Moureau, V., Fiorina, B., and Pitsch, H., A Level Set Formulation for Premixed Combustion LES Considering the Turbulent Flame Structure, *Combust. Flame*, **156**(4):801–812 (2009).

[110] Zhou, X. Y. and Pereira, J. C. F., Large Eddy Simulation (2D) of a Reacting Plane Mixing Layer using Filtered Density Function Closure, *Flow Turbul. Combust.*, **64**(4):279–300 (2000).

[111] Heinz, S., On Fokker-Planck Equations for Turbulent Reacting Flows. Part 1. Probability Density Function for Reynolds-Averaged Navier-Stokes Equations, *Flow Turbul. Combust.*, **70**(1–4):115–152 (2003).

[112] Raman, V., Pitsch, H., and Fox, R. O., Hybrid Large-Eddy Simulation/Lagrangian Filtered-Density-Function Approach for Simulating Turbulent Combustion, *Combust. Flame*, **143**(1–2):56–78 (2005).

[113] Raman, V. and Pitsch, H., Large-Eddy Simulation of a Bluff-Body-Stabilized Non-Premixed Flame using a Recursive Filter-Refinement Procedure, *Combust. Flame*, **142**(4):329–347 (2005).

[114] van Vliet, E., Derksen, J. J., and van den Akker, H. E. A., Turbulent Mixing in a Tubular Reactor: Assessment of an FDF/LES Approach, *AIChE J.*, **51**(3):725–739 (2005).

[115] Carrara, M. D. and DesJardin, P. E., A Filtered Mass Density Function Approach for Modeling Separated Two-Phase Flows for LES I: Mathematical Formulation, *Int. J. Multiphas. Flow*, **32**(3):365–384 (2006).

[116] Mustata, R., Valio, L., Jimnez, C., Jones, W., and Bondi, S., A Probability Density Function Eulerian Monte Carlo Field Method for Large Eddy Simulations: Application to a Turbulent Piloted Methane/Air Diffusion Flame (Sandia D), *Combust. Flame*, **145**(1–2):88–104 (2006).

[117] Jones, W. P., Navarro-Martinez, S., and Rohl, O., Large Eddy Simulation of Hydrogen Auto-Ignition with a Probability Density Function Method, *Proc. Combust. Inst.*, **31**(2):1765–1771 (2007).

[118] Jones, W. P. and Navarro-Martinez, S., Large Eddy Simulation of Autoignition with a Subgrid Probability Density Function Method, *Combust. Flame*, **150**(3):170–187 (2007).

[119] James, S., Zhu, J., and Anand, M. S., Large Eddy Simulation of Turbulent Flames Using the Filtered Density Function Model, *Proc. Combust. Inst.*, **31**(2):1737–1745 (2007).

[120] Chen, J.-Y., A Eulerian PDF Scheme for LES of Nonpremixed Turbulent Combustion with Second-Order Accurate Mixture Fraction, *Combust. Theor. Model.*, **11**(5):675–695 (2007).

[121] McDermott, R. and Pope, S. B., A Particle Formulation for Treating Differential Diffusion in Filtered Density Function Methods, *J. Comput. Phys.*, **226**(1):947–993 (2007).

[122] Raman, V. and Pitsch, H., A Consistent LES/Filtered-Density Function Formulation for the Simulation of Turbulent Flames with Detailed Chemistry, *Proc. Combust. Inst.*, **31**(2):1711–1719 (2007).

[123] Afshari, A., Jaberi, F. A., and Shih, T. I.-P., Large-Eddy Simulations of Turbulent Flows in an Axisymmetric Dump Combustor, *AIAA J.*, **46**(7):1576–1592 (2008).

[124] Drozda, T. G., Wang, G., Sankaran, V., Mayo, J. R., Oefelein, J. C., and Barlow, R. S., Scalar Filtered Mass Density Functions in Nonpremixed Turbulent Jet Flames, *Combust. Flame*, **155**(1–2):54–69 (2008).

[125] Réveillon, J. and Vervisch, L., Subgrid-Scale Turbulent Micromixing: Dynamic Approach, *AIAA J.*, **36**(3):336–341 (1998).

[126] Cha, C. M. and Trouillet, P., A Subgrid-Scale Mixing Model for Large-Eddy Simulation of Turbulent Reacting Flows using the Filtered Density Function, *Phys. Fluids*, **15**(6):1496–1504 (2003).

[127] Heinz, S., Unified Turbulence Models for LES and RANS, FDF and PDF Simulations, *Theor. Comp. Fluid Dyn.*, **21**(2):99–118 (2007).

[128] Tong, C., Measurements of Conserved Scalar Filtered Density Function in a Turbulent Jet, *Phys. Fluids*, **13**(10):2923–2937 (2001).

[129] Wang, D. and Tong, C., Conditionally Filtered Scalar Dissipation, Scalar Diffusion, and Velocity in a Turbulent Jet, *Phys. Fluids*, **14**(7):2170–2185 (2002).

[130] Rajagopalan, A. G. and Tong, C., Experimental Investigation of Scalar-Scalar-Dissipation Filtered Joint Density Function and its Transport Equation, *Phys. Fluids*, **15**(1):227–244 (2003).

[131] Wang, D., Tong, C., and Pope, S. B., Experimental Study of Velocity Filtered Joint Density Function for Large Eddy Simulation, *Phys. Fluids*, **16**(10):3599–3613 (2004).

[132] Wang, D. and Tong, C., Experimental Study of Velocity-Scalar Filtered Joint Density Function for LES of Turbulent Combustion, *Proc. Combust. Inst.*, **30**(1):567–574 (2005).

[133] Colucci, P. J., Large Eddy Simulation of Turbulent Reactive Flows: Stochastic Representation of the Subgrid Scale Scalar Fluctutations, Ph.D. Thesis, State University of New York at Buffalo, Buffalo, NY, 1998.

[134] Gicquel, L. Y. M., Velocity Filtered Density Function for Large Eddy Simulation of Turbulent Flows, Ph.D. Thesis, Department of Mechanical Engineering, State University of New York at Buffalo, Buffalo, NY, 2001.

[135] Drozda, T. G., Implementation of LES/SFMDF for Prediction of Non-Premixed Turbulent Flames, Ph.D. Thesis, Department of Mechanical Engineering, University of Pittsburgh, Pittsburgh, PA, 2005.

[136] Sheikhi, M. R. H., Joint Velocity Scalar Filtered Density Function for Large Eddy Simulation of Turbulent Reacting Flows, Ph.D. Thesis, Department of Mechanical Engineering, University of Pittsburgh, Pittsburgh, PA, 2005.

[137] Pisciuneri, P. H., Large Eddy Simulation of a Turbulent Nonpremixed Jet Flame Using a Finite-Rate Chemistry Model, M.S. Thesis, Department of Mechanical Engineering and Materials Science, University of Pittsburgh, Pittsburgh, PA, 2008.

[138] Yilmaz, S. L., RANS/PDF and LES/FDF for Prediction of Turbulent Premixed Flames, Ph.D. Thesis, Department of Mechanical Engineering and Materials Science, University of Pittsburgh, Pittsburgh, PA, 2008.

[139] Ansari, N., Filtered Density Function for Large Eddy Simulation of Turbulent Reacting Flows on Unstructured Meshes, Ph.D. Thesis, Department of Mechanical Engineering and Materials Science, University of Pittsburgh, Pittsburgh, PA, 2012.

[140] Otis, C. C., High-Fidelity Simulation of Compressible Flows for Hypersonic Propulsion Applications, Ph.D. Thesis, Department of Mechanical Engineering and Materials Science, University of Pittsburgh, Pittsburgh, PA, 2013.

[141] Pisciuneri, P. H., Yilmaz, S. L., Strakey, P. A., and Givi, P., An Irregularly Portioned FDF Simulator, *SIAM J. Sci. Comput.*, (2013), in press.

[142] Pisciuneri, P. H., Yilmaz, S. L., Strakey, P., and Givi, P., An Irregularly Portioned FDF Solver, *Bull. Am. Phys. Soc.*, **56**(18):305 (2011).

[143] Pisciuneri, P. H., Yilmaz, S. L., and Givi, P., Petascale FDF Large Eddy Simulation of Reacting Flows, *Bull. Am. Phys. Soc.*, **57**(17):123 (2012).

[144] Yilmaz, S. L., Ansari, N., Pisciuneri, P. H., Nik, M. B., Otis, C. C., and Givi, P., Advances in FDF Modeling and Simulation, in *47th AIAA/ASME/SAE/ASEE Joint Propulsion Conference & Exhibit*, pp. 1–11, San Diego, CA, 2011, AIAA, AIAA-2011-5918.

[145] Yilmaz, S. L., Ansari, N., Pisciuneri, P. H., Nik, M. B., Otis, C. C., and Givi, P., Applied Filtered Density Function, *J. Appl. Fluid Mech.*, **6**(3):311–320 (2013).

[146] Drozda, T. G., Quinlan, J. R., Pisciuneri, P. H., and Yilmaz, S. L., Progress Toward Affordable High Fidelity Combustion Simulations for High-Speed Flows in Complex Geometries, in *48th AIAA/ASME/SAE/ASEE Joint Propulsion Conference & Exhibit*, pp. 1–16, Atlanta, GA, 2012, AIAA, AIAA-2012-4264.

[147] Ansari, N., Pisciuneri, P. H., Strakey, P. A., and Givi, P., Scalar-Filtered Mass-Density-Function Simulation of Swirling Reacting Flows on Unstructured Grids, *AIAA J.*, **50**(11):2476–2482 (2012).

[148] Sagaut, P., *Large Eddy Simulation for Incompressible Flows*, Springer, New York, NY, third edition, 2010.

[149] Vreman, B., Geurts, B., and Kuerten, H., Realizability Conditions for the Turbulent Stress Tensor in Large-Eddy Simulation, *J. Fluid Mech.*, **278**:351–362 (1994).

[150] Erlebacher, G., Hussaini, M. Y., Speziale, C. G., and Zang, T. A., Toward the Large-Eddy Simulation of Compressible Turbulent Flows, *J. Fluid Mech.*, **238**:155–185 (1992).

[151] Bardina, J., Ferziger, J. H., and Reynolds, W. C., Improved Turbulence Models Based on Large Eddy Simulation of Homogeneous, Incompressible Turbulent Flows, Department of Mechanical Engineering Report TF-19, Stanford University, Stanford, CA, 1983.

[152] Eidson, T. M., Numerical Simulation of the Turbulent Rayleigh-Benard Problem using Subgrid Modeling, *J. Fluid Mech.*, **158**:245–268 (1985).

[153] Dopazo, C. and O'Brien, E. E., Statistical Treatment of Non-Isothermal Chemical Reactions in Turbulence, *Combust. Sci. Technol.*, **13**(1–6):99–122 (1976).

[154] Risken, H., *The Fokker-Planck Equation, Methods of Solution and Applications*, Springer-Verlag, New York, NY, 1989.

[155] Gardiner, C. W., *Handbook of Stochastic Methods for Physics, Chemistry and the Natural Sciences*, Springer-Verlag, New York, NY, second edition, 1990.

[156] Karlin, S. and Taylor, H. M., *A Second Course in Stochastic Processes*, Academic Press, New York, NY, 1981.

[157] Kloeden, P. E. and Platen, E., *Numerical Solution of Stochastic Differential Equations*, *Applications of Mathematics*, Vol. 23, Springer, Berlin; New York, third edition, 1999.

[158] MacCormack, R. W., The Effect of Viscosity in Hypervelocity Impact Cratering, *J. Spacecraft Rockets*, **40**(5):757–763 (2003).

[159] Gottlieb, D. and Turkel, E., Dissipative Two-Four Methods for Time-Dependent Problems, *Math. Comput.*, **30**(136):703–723 (1976).

[160] Peters, N., *Turbulent Combustion*, Cambridge University Press, Cambridge, UK, 2000.

[161] Pope, S. B., Computationally Efficient Implementation of Combustion Chemistry using *in situ* Adaptive Tabulation, *Combust. Theor. Model.*, **1**(1):41–63 (1997).

[162] Singer, M. A. and Pope, S. B., Exploiting ISAT to Solve the Reaction-Diffusion Equation, *Combust. Theor. Model.*, **8**(2):361–383 (2004).

[163] Liu, B. J. D. and Pope, S. B., The Performance of *in situ* Adaptive Tabulation in Computations of Turbulent Flames, *Combust. Theor. Model.*, **9**(4):549–568 (2005).

[164] Singer, M. A., Pope, S. B., and Najm, H. N., Modeling Unsteady Reacting Flow with Operator Splitting and ISAT, *Combust. Flame*, **147**(1–2):150–162 (2006).

[165] Singer, M. A., Pope, S. B., and Najm, H. N., Operator-Splitting with ISAT to Model Reacting Flow with Detailed Chemistry, *Combust. Theor. Model.*, **10**(2):199–217 (2006).

[166] Hiremath, V., Lantz, S. R., Wang, H., and Pope, S. B., Computationally-Efficient and Scalable Parallel Implementation of Chemistry in Simulations of Turbulent Combustion, *Combust. Flame*, **159**(10):3096–3109 (2012).

[167] Gourdain, N., Gicquel, L., Montagnac, M., Vermorel, O., Gazaix, M., Staffelbach, G., Garcia, M., Boussuge, J.-F., and Poinsot, T., High Performance Parallel Computing of Flows in Complex Geometries: I. Methods, *Comput. Sci. Disc.*, **2**:015003 (2009).

[168] Gropp, W., Lusk, E., and Skjellum, A., *Using MPI: Portable Parallel Programming with the Message-Passing Interface*, Scientific and Engineering Computation, MIT Press, Cambridge, MA, second edition, 1999.

[169] Karypis, G. and Kumar, V., A Fast and High Quality Multilevel Scheme for Partitioning Irregular Graphs, *SIAM J. Sci. Comput.*, **20**(1):359–392 (1999).

[170] Chen, Y.-C., Peters, N., Schneemann, G. A., Wruck, N., Renz, U., and Mansour, M. S., The Detailed Flame Structure of Highly Stretched Turbulent Premixed Methane-Air Flames, *Combust. Flame*, **107**(3):223–226 (1996).

[171] Mallampalli, H. P., Fletcher, T. H., and Chen, J. Y., Evaluation of CH_4/NO_x Reduced Mechanisms Used for Modeling Lean Premixed Turbulent Combustion of Natural Gas, *J. Eng. Gas Turb. Power*, **120**(4):703–712 (1998).

[172] Sandia National Laboratories, TNF Workshop Website, Piloted Jet Flames, http://www.sandia.gov/TNF/pilotedjet.html, 2013.

[173] Barlow, R. S. and Frank, J. H., Effects of Turbulence on Species Mass Fractions in Methane/Air Jet Flames, *Proc. Combust. Inst.*, **27**(1):1087–1095 (1998).

[174] Nooren, P. A., Versluis, M., van der Meer, T. H., Barlow, R. S., and Frank, J. H., Raman-Rayleigh-LIF Measurements of Temperature and Species Concentrations in the Delft Piloted Turbulent Jet Diffusion Flame, *Appl. Phys. B*, **71**(1):95–111 (2000).

[175] Sung, C. J., Law, C. K., and Chen, J.-Y., An Augmented Reduced Mechanism for Methane Oxidation with Comprehensive Global Parametric Validation, *Proc. Combust. Inst.*, **27**(1):295–304 (1998).

[176] Frenklach, M., Wang, H., Yu, C.-L., Goldenberg, M., Bowman, C., Hanson, R., Davidson, D., Chang, E., Smith, G., Golden, D., Gardiner, W., and Lissianski, V., GRI-Mech 1.2, http://diesel.me.berkeley.edu/~gri_mech/new21/version12/text12.html, 2013.

[177] Frenklach, M., Wang, H., Goldenberg, M., Smith, G., Golden, D., Bowman, C., Hanson, R., Gardiner, W., and Lissianski, V., GRI-Mech—An Optimized Detailed Chemical Reaction Mechanism for Methane Combustion, Technical report, Gas Research Institute, 1995, Report No. GRI-95/0058.

[178] Xu, J. and Pope, S. B., PDF Calculations of Turbulent Nonpremixed Flames with Local Extinction, *Combust. Flame*, **123**(3):281–307 (2000).

[179] Yoo, C. S., Sankaran, R., and Chen, J. H., Three-Dimensional Direct Numerical Simulation of a Turbulent Lifted Hydrogen Jet Flame in Heated Coflow: Flame Stabilization and Structure, *J. Fluid Mech.*, **640**:453–481 (2009).

[180] Grout, R. W., Gruber, A., Yoo, C. S., and Chen, J. H., Direct Numerical Simulation of Flame Stabilization Downstream of a Transverse Fuel Jet in Cross-Flow, *Proc. Combust. Inst.*, **33**(1):1629–1637 (2011).

[181] Boman, E., Devine, K., Heaphy, R., Hendrickson, B., Leung, V., Riesen, L. A., Vaughan, C., Catalyurek, U., Bozdag, D., Mitchell, W., and Teresco, J., *Zoltan 3.0: Parallel Partitioning, Load Balancing, and Data-Management Services; User's Guide*, Sandia National Laboratories, Albuquerque, NM, 2007, Tech. Report SAND2007-4748W http://www.cs.sandia.gov/Zoltan/ug_html/ug.html.

[182] Karypis, G. and Schloegel, K., *ParMETIS: Parallel Graph Partitioning and Sparse Matrix Ordering Library, Version 4.0*, University of Minnesota, Minneapolis, MN, 2013.

[183] OpenMP Architecture Review Board, The OpenMP API Specification for Parallel Programming, http://openmp.org/wp/, 2013.